PHYSICAL REVIEW B VOLUME 25, NUMBER 2 15 JANUARY 1982

Motion of defects and stress relaxation in two-dimensional crystals

R. Bruinsma
Department of Physics, Harvard University, Cambridge, Massachusetts 02138
and Brookhaven National Laboratory, Upton, New York 11973*

B. I. Halperin
Department of Physics, Harvard University, Cambridge, Massachusetts 02138

Annette Zippelius
Department of Physics, Harvard University, Cambridge, Massachusetts 02138
and Laboratory of Atomic and Solid State Physics, Cornell University, Ithaca, New York 04853*
(Received 5 March 1981)

The stress relaxation of a two-dimensional solid is studied, with the assumption that defects have been trapped in the sample. The effective shear modulus and stress-strain relaxation rate are calculated for a variety of defect configurations, including large- and small-angle grain boundaries and dislocation pairs. Effects of dislocation climb on the long-term stability of the configurations are considered. The viscosity resulting from moving free dislocations and/or flow at the boundaries is described in a particular geometry. The response to a finite applied shear is discussed, in particular, nucleation of free dislocations and sliding of grain boundaries. The theory is applied to free-standing smectic-*B* films, and it is suggested that stress relaxation observed in these films may result from a dilute "random neutral array" of dislocations or from small-angle grain boundaries.

I. INTRODUCTION

There is considerable interest, at present, in measurements of the elastic constants of quasi-two-dimensional systems near a melting transition.[1,2] One set of experiments[2] has obtained values for the shear elastic constants in very thin films of the liquid crystal N-(4-*n*-butyloxybenzylidene)-4-*n*-octylaniline (40.8) near the transition from the smectic-*B* to smectic-*A* phases. It has been confirmed by x-ray measurements[3] that the smectic-*B* phase in this material is a highly anisotropic, layered solid, while the *A* phase may be considered to be a stack of two-dimensional liquids. The elasticity measurements, which were made at a frequency of order 10^3 Hz, showed that the shear modulus per molecular layer at a temperature below the bulk $B-A$ transition has a value which is in the general vicinity of the value one would estimate from the Kosterlitz-Thouless[4,5] theory of two-dimensional melting.

In order to study the elastic constants at lower frequencies, Sprenger *et al.*[6] have measured the behavior of the stress over a period $\lesssim 10^3$ sec after a step-function change in the macroscopic strain. In the course of this measurement period, the experimenters observe slippage or stress relaxation in the film even at temperatures well into the smectic-*B* (solid) phase. This stress relaxation appears to be very nonexponential, with relaxation slowing down drastically as time proceeds. The relaxation times depend strongly on the thickness of the film (e.g., $\tau \simeq 0.01$ sec for four-layer films, $\tau \simeq 1000$ sec for 25 layers), and the strain becomes nonlinear for rather small values of the applied stress. Nonexponential relaxation is observed, however, even in the linear regime.

Important relaxation effects were also observed by Tarczon and Miyano[2] in the frequency range $0.25-80$ Hz in ac measurements of the shear modulus of 40.8 films in the smectic-*B* region. If the smectic-*B* phase is indeed a layered solid, then the observed stress relaxation must be due to the presence of defects in the sample. In order to understand these experiments, it is then necessary to understand the nature of defects that may be present and to understand how these defects will respond to a low-frequency stress.

Although a certain density of tightly bound dislocation pairs is expected in a two-dimensional

solid in thermal equilibrium,[5] the response of such pairs to an applied stress would be too small and too rapid to account for the observed relaxations.[7] Consequently, we shall focus our attention on the behavior of a nonequilibrium "quenched" array of defects. The quenched-in distribution of defects must be sufficiently stable to last for the duration of the experiment[6] (say, 10^3 sec), unless defects are being continually injected due to some unknown motion at the boundaries. On the other hand, the defects must be sufficiently mobile to respond on the time scales of the observed stress relaxation ($0.01-10^3$ sec).

In this paper we shall examine the stability of some simple defect arrays that may occur in a two-dimensional solid and analyze their time-resolved response to an applied stress. The possible application to the liquid-crystal experiments, which are on films of more than one layer, will be discussed in our final section.

Most of the defects considered in this paper are collections of dislocations,[8] with separations that are large compared to the lattice constant. The dislocations may be organized into low-angle grain boundaries,[9] or may be more nearly random in the plane. We shall only consider arrays which are at least metastable with regard to glide of the dislocations (i.e., motion parallel to the Burgers vector). However, we do not require stability with regard to dislocation climb (motion perpendicular to the Burgers vector). In general, climb is much slower than glide, since interstitials or vacancies are necessary for the process. The rate of climb is not zero, however, as some equilibrium concentrations of interstitials and vacancies must inevitably be present, particularly when one is close to the melting point.

As a very rough estimate, we shall assume the diffusion constant for dislocation glide in a single molecular layer to be of the order of 10^{-6} cm^2/sec, comparable to the diffusion constant for a vacancy at the melting temperature of a solid,[10,11] or the diffusion constant of a molecule in a liquid.[12] We shall guess that the vacancy or interstitial concentration is of the order of 10^{-4},[11] and that the diffusion constant for climb is thus of the order of 10^{-10} cm^2/sec. We shall see that this diffusion constant is still sufficiently large to place important constraints on the minimum separation between dislocations of opposite sign.

Recently, there have been several attempts to test the theory of two-dimensional (2D) melting in molecular dynamics studies and Monte Carlo simulations.[13] The latter seem to indicate that close to the melting transition extremely long runs are necessary to establish thermodynamic equilibrium. Our analysis of the behavior of "quenched-in" defects suggests possible mechanisms which considerably delay the relaxation to equilibrium. In particular, our calculation of time scales, necessary to annihilate nonequilibrium defects such as small-angle grain boundaries, might serve as an estimate for the time scales of a numerical simulation of a solid, cooled down rapidly from the liquid phase.

Many of the discussions in this paper are similar to considerations which are well known in the theory of defect motion in three-dimensional crystals.[8] There are, however, important differences between two and three dimensions. Some three-dimensional phenomena, such as the bending of a dislocation line, have no direct counterpart in two dimensions. In general, the pinning of dislocations will be quite different in the two cases.

In three dimensions, dislocations are typically pinned by a conglomeration of point defects or impurities, by entanglement with other dislocations, or by some similar mechanism. The resulting barriers to dislocation motion are generally large compared to k_BT, and cannot be overcome by simple thermal activation. Instead, the barriers must be overcome by the application of an external force, which leads immediately to strong nonlinearities in response to applied strain. The sensitivity to applied stress is increased also in the three-dimensional case by the phenomenon of stress enhancement that occurs when a dislocation line is pinned only at isolated points along its length.

In two dimensions, by contrast, the maximum pinning energy for a dislocation at a localized defect or at a collection of impurities will generally be of the order of a few times k_BT for temperatures near to the melting temperature, as discussed in Sec. II B below. (Somewhat larger barriers may occur in a multilayered sample.) Thus simple thermal motion is enough to overcome local pinning of an individual dislocation. Relatively stable configurations and long relaxation times can be obtained due to collective effects and/or large separations between dislocations.

A detailed discussion of the manner in which dislocations first become trapped in the sample is beyond the scope of this paper. It seems likely that the dislocations are trapped as the film is cooled through the freezing temperature ($A \rightarrow B$ transition) just as dislocations are formed in melt-grown three-dimensional solids. For example, precipitation of vacancies[14] in close-packed crystal

planes causes formation of edge dislocations, which close to T_m then may form rapidly into grain-boundary networks. Just as in three dimensions, dislocations tend to be trapped in grain boundaries.[15]

Alternatively, dislocations might be formed to relieve large stresses due to boundary conditions on the crystal orientation. Dislocations in a bent crystal will tend to arrange themselves in grain boundaries along the radius of curvature (polygonization).[16] The formation of grains in this way is a two stage process: First glide, then climb (coarsening). An example will be given in Sec. IV.

Since the particular types of defects present in the experimental samples are not known, and since in any case the trapped defects may be different in future samples prepared by different means, we shall attempt in this paper to discuss a variety of defect configurations that might be important under one or another circumstance. Which defects are important for dissipation may depend not only on the sample preparation and geometry, but also on conditions of measurement, such as the magnitude and application rate of the applied stress. A summary of the mechanisms discussed in this paper, and some estimates of the associated relaxation times are summarized in Table I.

The relaxation mechanisms discussed in this paper are of two types. For some defect arrays, including most of those discussed in Secs. II and III, the defects lead to a low-frequency renormalized shear modulus μ_R, which is reduced to a finite fraction (possibly small) of the high-frequency (microscopic) shear modulus μ. The relaxation times discussed in these sections are then the time scales necessary to see the low-frequency modulus or, equivalently, the time necessary for the maximum strain to develop under constant stress. This relaxation may be said to be recoverable, as the sample will eventually return to its original shape if the stress is removed.

In other examples, as in Secs. V and VI, we are concerned with "nonrecoverable" relaxation, i.e., situations where the static (dc) shear modulus is zero. Here the system may be described by an effective viscosity η, and the relaxation time τ determined by the ratio of the viscosity to the high-frequency shear modulus μ (sometimes called the Maxwellian relaxation time) describes the time for relaxation of stress after imposition of a given macroscopic strain. Alternatively, in a time-dependent (ac) experiment the characteristic frequency $\omega_0 \sim 1/\tau$ determines the crossover from viscous behavior at low frequencies to elastic behavior at high frequencies. Both recoverable and nonrecoverable relaxation may occur in the experiments on smectic films.

Outline

The organization of the paper is as follows. In Sec. II we consider some defects which are built up out of separated dislocations— in particular, small-angle grain boundaries and isolated, well-separated dislocation pairs. We discuss the effect of dislocation glide motion on the measured shear modulus and the strain relaxation rate. Here we assume that the grain boundaries are pinned at isolated points—e.g., at the intersections of boundaries, or at the intersection with the boundary of the sample. We also investigate, in Sec. II C, the rate at which small-angle grain boundaries can disappear in the presence of a finite climb rate, and we use this analysis to estimate the minimum allowable dislocation separations that could persist for long times in a two-dimensional sample.

As the opposite of small-angle grain boundaries, one can consider a sample made up of crystallites separated by large-angle grain boundaries. Stress relaxation due to slip in a network of large-angle grain boundaries is considered in Sec. III.

When a two-dimensional crystal is formed, conditions at the boundary of the sample may force the crystal axes, locally, to assume a particular orientation relative to the boundary. In the case of a circular boundary, or an annular geometry, such a boundary condition would clearly result in a bent-crystal sample, unless dislocations or grain boundaries are formed to relieve the stress. The geometric arrangement of the resulting stable dislocation array is discussed in Sec. IV. In Sec. V, we summarize the relaxation of stress due to motion of free dislocations, or of arrays of dislocations such as those that would be encountered in the bent-crystal geometry of Sec. IV.

Another mechanism for stress relaxation occurs if there is a thin liquid band between the boundary of the sample and the rigid containing wall. If the wall is rough, slippage of the sample relative to the wall requires melting at points of high compression and flow of matter through the liquid band to a region of low compression, where resolidification occurs. This process is analyzed in Sec. VI.

The relaxation processes described so far have been primarily linear processes, where the relaxa-

TABLE I. Time scales of stress relaxation in a two-dimensional solid. The numerical estimates are appropriate for a smectic-B solid monolayer, with a film thickness $h=30$ Å. Definitions of parameters and their numerical values assumed for the time estimates are as follows. Lattice constant $a_0 \simeq 5$ Å, shear modulus $\mu \approx 200$ erg/cm^2, and $T \approx 300$ K, so that the reduced elastic constant $\bar{K}$ is close to Kosterlitz-Thouless critical value ($\bar{K} \approx 4$), with $\bar{K} \equiv (\mu a_0^2/\pi k_B T) \times [(\mu+\lambda)/(\mu+2\lambda)]$; glide diffusion constant for dislocations $D_{\|} \approx 10^{-6}$ cm^2/sec; climb diffusion constant $D_{\perp} \approx 10^{-10}$ cm^2/sec; dislocation core energy E_c and barrier heights ΔE are of the order of $k_B T$ for a single-layer film; assumed smectic-A liquid region at sample boundary or at large-angle grain boundary has width $w \approx 5$ Å and viscosity $\eta = 0.1$ poise; dislocation separation in small-angle grain boundary, $d \approx 100$ Å; separation of dislocation pair or dislocation separation in random neutral array, $r \approx 10^4$ Å; grain size $L \approx 1$ mm; sample has annular geometry shown in Fig. 8, with $R=1$ cm and $\Delta R = 1$ mm. Containing boundaries are assumed to have irregularities, with typical height $l \approx 10^{-4}$ cm. The shear strains u_{xy} used in the experiments of Ref. 6 were typically in the range $10^{-6}-10^{-4}$. Processes marked with an asterisk are thermally activated, and their time scales should increase exponentially with the number of layers n in a multilayer film, e.g., the exponents $\Delta E/k_B T$ and $\bar{K}$ may be estimated as $0.6n$ and $4n$, respectively, for some range of n. The remaining, nonactivated processes should be only weakly dependent on film thickness.

Process	Approximate time scale for single layer film (sec)
Linear recoverable relaxation	
Glide of pinned small-angle grain boundary [Eq. (2.22b)]	$\tau = Ld/4\pi^2 D_{\|} \sim 10^{-3}$
Slip in a large-angle grain boundary network [Eq. (3.7)]	$\tau = \eta L h/\mu w \sim 10^{-4}$
Nonlinear, recoverable relaxation	
Glide of widely separated dislocation pairs* [Eq. (2.44)]	$\tau \simeq \frac{r^2}{D_{\|}} e^{\Delta E_0/k_B T} \sim 10^{-2}$*
Linear nonrecoverable relaxation	
Climb of widely separated dislocation pairs [Eq. (2.54)]	$\tau = r^2/D_{\perp} \sim 10^2$
Climb of small-angle grain boundaries [Eq. (2.41)]	$\tau \simeq L^2/D_{\perp} \sim 10^8$
Glide of dislocations in a bent crystal [Eq. (5.4)]	$\tau \simeq R k_B T/a_0 \mu D_{\|} \sim 10^{-2}$
Flow at the sample boundary [Eq. (6.10)]	$\tau = 12\eta h l^2 \Delta R/w^3 \mu \sim 10^4$
Nonlinear, nonrecoverable relaxation	
Pair dissociation*	$\tau \simeq \frac{3a_0^2 \bar{K}^{1/2}}{D_{\|}} \left[\frac{k_B T}{2\mu a_0^2}\right]^{1+\bar{K}/2} \frac{e^{E_c/k_B T}}{(u_{xy})^{\bar{K}/2}} \sim \frac{10^{-13}}{u_{xy}^2}$*
Escape from small-angle grain boundary* [Eq. (7.40)]	$\tau = \frac{0.3d^2}{D_{\|}} \left[\frac{e^{-2\bar{K}}}{\bar{K}(\bar{K}-1)}\right] \left[\frac{a_0}{u_{xy} d}\right]^{1+\bar{K}} \sim \frac{10^{-17}}{u_{xy}^5}$*
Depinning time for intersecting small-angle grain boundaries* (Sec. VII C)	$\tau = \frac{d^2}{D_{\|}} e^{\Delta E/k_B T} \sim 10^{-6}$*
Thermally activated glide in a "random neutral array" of dislocations* (Sec. VIII)	$\tau = \frac{r^2}{D_{\|}} e^{\Delta E/k_B T} \sim 10^{-2}$*

tion times are independent of the stress for small stresses. There are, however, a variety of nonlinear processes which may be important at relatively small stresses in a two-dimensional sample. In Sec. VII A, we discuss the stress-induced dissociation of dislocation pairs, which can be present even in true thermal equilibrium in a two-dimensional sample. In Sec. VII B, we discuss an analogous process, the stress-induced "evaporation" of a dislocation from a small-angle grain boundary. Then, in Sec. VII C we discuss sliding of two intersecting small-angle grain boundaries, taking into account the tendency for the grain boundaries to become pinned at local minima (with respect to glide) of the energy of interaction between the dislocation in the two grain boundaries. Again, the nonlinear effects of applied stress are considered.

Finally, in Sec. VIII, we discuss application of the previous analyses to the case of a multilayer smectic-*B* (crystalline) film. Many of the relaxation processes can be eliminated from consideration as the source of the experimentally observed stress relaxation because they do not lead to effects of significant magnitude on the correct time scale. Likely candidates, however, are a network of small-angle grain boundaries or a dilute "random neutral array" of dislocations. A random neutral array may be considered as a generalization of a dislocation pair to an infinite array in which each dislocation is interacting with several nearby dislocations of different Burgers vectors. Alternatively, the array may be considered to be a network of very small-angle grain boundaries in which the distance between grain boundaries is comparable to the distance between dislocations in the grain boundary. In any case, the required distances between dislocations are found to be quite large. (See Table I).

II. METASTABLE DISLOCATION STRUCTURES

In this section we discuss two defect configurations built up out of dislocations: small-angle grain boundaries and widely separated dislocation pairs. In order to understand the relaxation of these defects, it is important to note that two time scales are associated with the motion of dislocations. A dislocation can *glide*, i.e., move parallel to its Burgers vector, and *climb*, i.e., move perpendicular to its Burgers vector.[17] The latter can only proceed by the emission or absorption of vacancies or interstitials, while dislocation glide does not involve a net change in particle density. Therefore, climb is, in general, a much slower process than glide. If the concentration of vacancies and interstitials is low—as we expect to be the case even near the melting temperature—climb is strongly inhibited. Then defect configurations, which can only relax by dislocation climb, are stable over very long time scales, i.e., as long as climb does not take place appreciably. We first discuss the effect of such metastable defects on the static and dynamic properties of a 2D solid, assuming that dislocation climb is not allowed. We then consider dislocation climb and calculate the lifetimes of these defect structures.

A. Small-angle grain boundary

Our first example is a pinned, small-angle grain boundary, which can be deformed under an applied shear and thereby reduce the shear modulus.[18] Possible pinning mechanisms will be discussed in Secs. II B and II C. A small-angle grain boundary can be considered a line of dislocations with equal Burgers vectors $\vec{b}$. In the configuration of lowest energy the Burgers vectors are of minimum size, equally spaced, and perpendicular to the grain boundary.[19] In order to have zero net macroscopic dislocation density we consider two parallel grain boundaries a distance D apart and with opposite Burgers vectors. Each boundary is assumed to be pinned at the ends, L being the distance between the pinning centers. The domains separated by the grain boundaries are tilted by an angle θ with respect to each other. θ is related to the distance d between dislocations, $\theta=a_0/d$, where a_0 denotes the lattice spacing. If the number N_0 of dislocations between two pinning centers is large, one can easily calculate the energy of the two straight, parallel grain boundaries[19,20] for large L,

$$E=\frac{Ka_0^2}{8\pi}\sum_{i\neq j}\left[-\vec{b}_i\cdot\vec{b}_j\ln\frac{|\vec{r}_{ij}|}{a_0}+\frac{(\vec{b}_i\cdot\vec{r}_{ij})(\vec{b}_j\cdot\vec{r}_{ij})}{|\vec{r}_{ij}|^2}\right]+E_c\sum_i\vec{b}_i^2\,, \tag{2.1a}$$

giving

$$\frac{E}{N_0}=2E_c+\frac{Ka_0^2}{4\pi}\left[\ln\frac{d}{2\pi a_0}-\frac{\pi D}{d}\coth\frac{\pi D}{d}+\ln\left[2\sinh\frac{\pi D}{d}\right]\right]\,, \tag{2.1b}$$

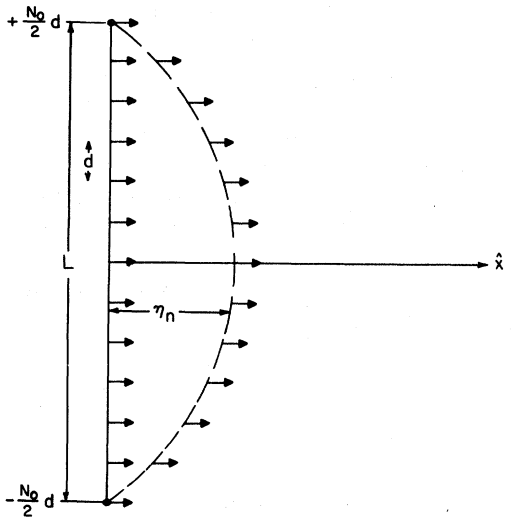

FIG. 1. Initial and final position of a grain boundary when shear stress is applied. The N_0 dislocations are initially along the y axis, separated by d and pinned at $y=\pm(N_0/2)d$. Their final positions are indicated by η_n. Here and in all other figures, we represent dislocations by their Burgers vectors, indicated by arrows.

where E_c denotes the core energy of a dislocation and K is a particular combination of the Lamé coefficients μ and λ, $K=4\mu(\mu+\lambda)/(2\mu+\lambda)$. In the limit $D\to\infty$, one finds

$$\frac{E}{N_0}=2E_c+\frac{Ka_0^2}{4\pi}\ln\frac{d}{2\pi a_0}-\frac{Ka_0^2D}{2d}e^{-2\pi D/d}, \tag{2.2}$$

so that one can define the energy of one grain boundary

$$\frac{E_{\rm GB}}{N_0}=E_c+\frac{Ka_0^2}{8\pi}\ln\frac{d}{2\pi a_0}. \tag{2.3}$$

In the following we will assume that the density of grain boundaries is low, i.e., $D>>L$, so that we can neglect interactions between different boundaries.

We are interested in deformations of a pinned grain boundary under an applied stress field, assuming that dislocations can only glide. For definiteness, we consider a grain boundary along the y axis with N_0 dislocations (Fig. 1). The Burgers vectors $\vec{b}_n=\binom{1}{0}$ can glide along the $\hat{x}$ direction, so that a possible deformation is described by the positions of the dislocations $\vec{r}_n=nd\hat{y}+\eta_n\hat{x}$, where η_n denotes the deviations from the straight-line configuration. We expand the line energy up to quadratic terms in η_n and find for the energy of deformation

$$\delta E=\frac{Ka_0^2}{16\pi}\sum_{n\neq m}\frac{(\eta_n-\eta_m)^2}{(n-m)^2d^2}. \tag{2.4}$$

If a shear $\vec{\vec{\sigma}}=\begin{pmatrix}0&\sigma\\ \sigma&0\end{pmatrix}$ is applied, the dislocations would like to glide in such a way as to relax the stress. Their motion is opposed by friction and the restoring force of the grain boundary. The resulting equation of motion is

$$\gamma_{||}\dot{\eta}_n+\frac{\delta E}{\delta\eta_n}=a_0\sigma, \tag{2.5}$$

where $\gamma_{||}$ is a phenomenological friction coefficient for glide.

We first calculate the static displacement as the solution of

$$\frac{\delta E}{\delta\eta_n}=\sum_m V_{nm}\eta_m=a_0\sigma, \tag{2.6}$$

where

$$V_{nm}=\begin{cases}-\dfrac{Ka_0^2}{4\pi d^2}\dfrac{1}{(n-m)^2}, & n\neq m\\ \dfrac{Ka_0^2}{4\pi d^2}\displaystyle\sum_{k\neq n}\dfrac{1}{(n-k)^2}, & n=m.\end{cases} \tag{2.7}$$

This equation can be solved if the eigenvalues λ_l and eigenfunctions $\gamma_n^{(l)}$ of the matrix V_{nm}

$$\sum_m V_{nm}\gamma_m^{(l)}=\lambda_l\gamma_n^{(l)} \tag{2.8}$$

are known. For large, even N_0 it is straightforward to show

$$\gamma_n^{(l)}=\begin{cases}\sqrt{2/N_0}\cos\dfrac{\pi ln}{N_0}, & l=1,3,\ldots,N_0-1\\ \sqrt{2/N_0}\sin\dfrac{\pi ln}{N_0}, & l=2,4,\ldots,N_0\end{cases} \tag{2.9}$$

and

$$\lambda_l=\frac{\pi^2 l}{N_0}\frac{Ka_0^2}{4\pi d^2}\propto\frac{1}{L}. \tag{2.10}$$

The eigenfunctions vanish for $n=\pm N_0/2$, where the grain boundary is assumed to be pinned. From Eqs. (2.6)–(2.10) the displacement follows as

$$\eta_n=a_0\sigma\sum_m(V^{-1})_{nm}=a_0\sigma\sum_{m,l}\lambda_l^{-1}\gamma_n^{(l)}\gamma_m^{(l)}, \tag{2.11}$$

$$\eta_n=\frac{16\sigma Ld}{\pi^2 K a_0}\sum_{\text{odd}\,l}\frac{(i)^{l-1}}{l^2}\cos\frac{\pi l n}{N_0}\ . \tag{2.12}$$

The displacement grows linearly with the total length L of the grain boundary and therefore the deformation energy, given by

$$\delta E=\sum_{n,m}V_{nm}\eta_n\eta_m=\frac{32\sigma^2L^2}{K\pi^3}\zeta(3)\ , \tag{2.13}$$

with

$$\zeta(3)=\sum_{l=0}^{\infty}\frac{1}{(2l+1)^3}\approx 1.202\ , \tag{2.14}$$

is proportional to L^2. This is characteristic of the long-ranged logarithmic interaction between dislocations and is to be contrasted with a short-ranged interaction, which gives rise to a line energy like that, for example, in a 3D dislocation line.

The motion of dislocations leads to a change in shape of the sample which may be described by the macroscopic strain given by

$$U_{xy}=-\frac{a_0}{2}\sum_n\eta_n/A\ , \tag{2.15}$$

where A is the area of the sample. Assuming a uniform density of grain boundaries of length L, i.e., $n_0(L)=1/LD$, the total shear strain is given by

$$U_{xy}=\frac{\sigma}{2\mu}+\frac{a_0}{2}\frac{1}{LD}\sum_n\eta_n\ . \tag{2.16}$$

Using the stress-strain relation, we can define an effective shear modulus in the presence of grain boundaries,

$$\sigma=2\mu_{\text{eff}}U_{xy}=2(\mu-\delta\mu)U_{xy}\ , \tag{2.17}$$

which is reduced as compared to the perfect lattice by an amount

$$\frac{\delta\mu}{\mu}=\frac{8\zeta(3)}{\pi^3}\frac{L}{D}\frac{2\mu+\lambda}{\mu+\lambda}\ . \tag{2.18}$$

If the spacing D between grain boundaries is comparable to the length L of a free segment, then the reduction in μ can be of order 50%.

If the stress is switched off at $t=0$, the deformation will relax according to the equation of motion

$$\gamma_{||}\dot{\eta}_n+\sum_m V_{nm}\eta_m=0\ , \tag{2.19}$$

subject to the inital condition that $\eta_n(t=0)$ be given by (2.12). The coefficient $\gamma_{||}$ is a friction coefficient for dislocation glide. Since a dislocation is a pointlike object in two dimensions, we may use the Einstein relation to write

$$\gamma_{||}=k_BT/D_{||}\ , \tag{2.20}$$

where $D_{||}$ is the diffusion constant for dislocation glide and is typically determined by the process of activation over the barrier between minimum energy positions of the dislocation in adjacent unit cells. We have estimated this diffusion constant as being of the order of 10^{-6} cm^2/sec, for purposes of illustration. In an impure crystal, the diffusion rate may be reduced by the tendency of dislocations to be temporarily trapped at the sites of impurities or clusters of impurities. However, as discussed in Sec. II B below, the pinning energy for a dislocation at an impurity site should not be very large compared to k_BT near melting, so there will not be a drastic reduction of $\gamma_{||}$ in this case. Furthermore, an individual impurity itself can diffuse, or be dragged along by the dislocation, with a diffusion constant of the order of 10^{-6}.

To solve Eq. (2.19), we make the ansatz $\eta_n\sim e^{-\omega t}$. It then follows from (2.19) that $\omega\gamma_{||}$ must be an eigenvalue of the matrix V_{nm}. We therefore expand the general solution of (2.19) in the eigenfunctions of V_{nm},

$$\eta_n(t)=\sum_i A_i\exp(-\lambda_i t/\gamma_{||})\gamma_n^{(i)}\ , \tag{2.21a}$$

and determine the coefficients A_i from the initial condition

$$\eta_n(t)=\frac{16}{\pi^2K}\frac{d}{a_0}L\sigma\sum_{\text{odd}\,l}\cos\frac{\pi l n}{N_0}\frac{(i)^{l-1}}{l^2}\times\exp\left[-\frac{Ka_0^2}{4\pi d}\frac{\pi^2 l}{L\gamma_{||}}t\right]\ . \tag{2.21b}$$

We see that the relaxation of the displacement $\eta_n(t)$ is described by the superposition of many exponentials. The corresponding relaxation times decrease linearly with l, $\tau_l\sim 1/l$, so that for $t>(4\pi\gamma_{||}/Ka_0^2)\,(Ld/\pi^2)$ the decay will be dominated by the smallest eigenvalue

$$\tau_0^{-1}=\frac{Ka_0^2}{4\pi}\frac{\pi^2}{Ld\gamma_{||}} \tag{2.22a}$$

$$\simeq\frac{4\pi^2D_{||}}{Ld}\ . \tag{2.22b}$$

In (2.22b) we have replaced K by its value at T_c and used (2.20). For a grain boundary of length

$L \sim 1$ mm with a dislocation spacing of $d \sim 100$ Å and the glide diffusion constant $D_{\|} \sim 10^{-6}$ cm^2/sec, we find $\tau_o \sim 10^{-2}$ sec.

In a quenched system we expect to find grain boundaries of different lengths L, so that the single relaxation time τ_0 should be replaced by a distribution of decay times, depending continuously on L. In such a sample measurements of the stress relaxation will show a complicated time dependence with a pronounced delay in the total decay time, as shown above.

So far we have neglected interactions between different grain boundaries. If these are taken into account, one finds corrections of the order of L/D, so that our results may be regarded as the lowest-order term in a systematic expansion in L/D, which we assumed to be small.

B. Pinning

In two dimensions, a dislocation cannot be pinned down by a point defect except at low temperatures.[21] This can be illustrated as follows. The displacement field $\vec{u}$ of a vacancy at the origin in a two-dimensional crystal is given by

$$\vec{u} = \frac{a^2(x,y)}{x^2+y^2} , \tag{2.23}$$

here $2\pi a^2$ is the difference in area of a site occupied by a regular atom and a vacancy. Hence the length scale a is of the order of the lattice spacing a_0. A dislocation with Burgers vector $\vec{b}$ along x, moving in the glide plane $y=-D$, will feel a force F_x:

$$F_x = -a_0\sigma_{xy} = -4\mu a_0^3 \frac{xD}{(x^2+D^2)^2} . \tag{2.24}$$

To escape from this potential well the dislocation needs an energy ΔU:

$$\Delta U = -\int_0^\infty F_x dx = 2\mu \frac{a_0^3}{D} . \tag{2.25}$$

In the theory of two-dimensional melting[5] it is shown that $(4\pi)^{-1}\mu a_0^2 = k_B T_c$ so a dislocation can escape by thermal activation from a point singularity. In *three* dimensions a dislocation line can contain many point defects and generally cannot be depinned by thermal activation.[21] A *grain boundary* in *two* dimensions can likewise contain many point defects. In that case we expect a critical shear stress to dislodge it.

Possible pinning centers for a grain boundary can also be provided by the surface[22] of the sample. If the surface is not flat but contains, say, a step, then, as in three dimensions, we may expect that this aids in the nucleation as well as pinning of dislocations. If a grain boundary stretches across a sample as in a bicrystal, then it can be pinned by surface irregularities, which allow it to have the shortest length and therefore the smallest line tension. If the inhomogeneities of the surface are of size Δx then the pinning energy is roughly $\epsilon\Delta x$, where $\epsilon = E_{GB}/N_0 d$ is the line energy of the grain boundary [see Eq. (2.3)].

At the surface of the sample a boundary condition might be imposed on the orientation of the crystal axis. Depending on the geometry of the sample and the strength of the orienting force of the surface, it can be favorable to create a high-angle grain boundary which is locally parallel to the surface. We will discuss an example of such a process for a particular geometry in Sec. IV.

C. Example of a metastable configuration

In this section we investigate a simple configuration of pinned grain boundaries, which is stable as long as dislocation climb does not take place. We show that the topology of the grain provides an effective pinning mechanism and calculate the lifetime of the configuration being relaxed by dislocation climb.[23]

Let us consider a square lattice and for simplicity a square grain, as shown in Fig. 2. We require that the crystal inside the grain be undistorted. Then the dislocation density along each of the four boundaries of the grain must be the same. The

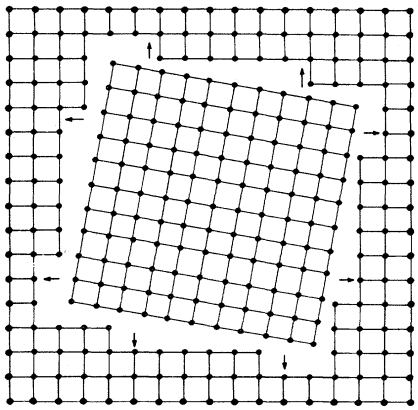

FIG. 2. A square grain with two dislocations per side. The Burgers vectors of the dislocations are indicated by arrows.

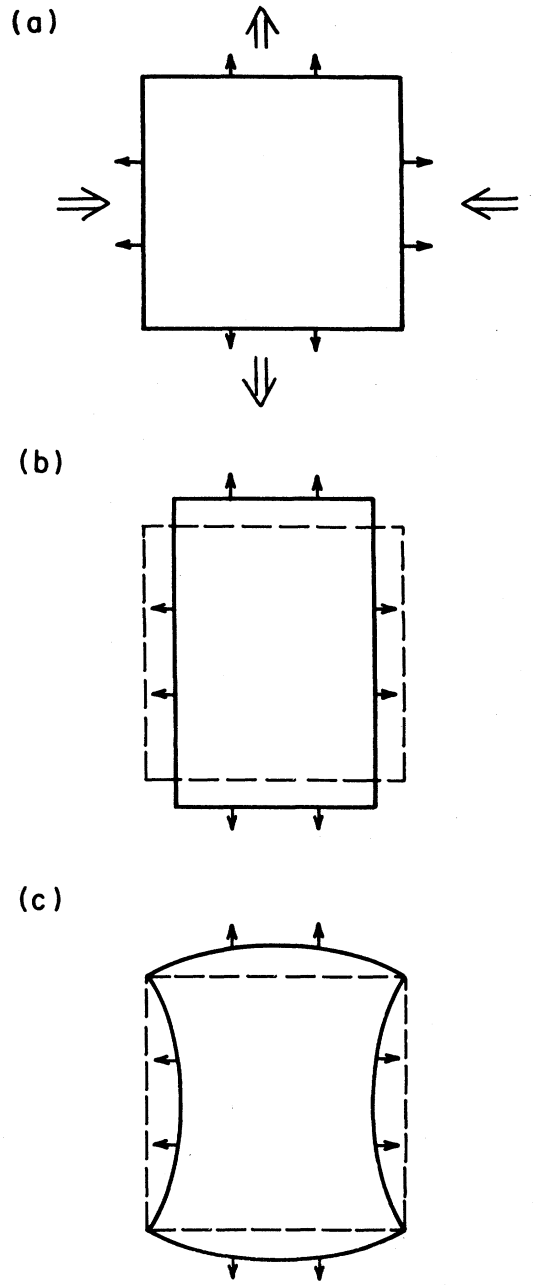

FIG. 3. Possible deformations of a square grain boundary under a uniform shear stress if climb is excluded. (a) shows the direction of the force exerted by the shear along the glide plain of the dislocations. (b) shows a grain boundary deformation (solid lines) which is not favorable due to deformations of the grain itself. (c) shows the actual grain boundary deformation (solid lines).

configuration shown in Fig. 2 has the same number of atoms as the lattice without grain; in particular, there are no interstitials or vacancies at the corners of the grain. If a shear $\overleftrightarrow{\sigma}=\begin{pmatrix}0 & \sigma\\ \sigma & 0\end{pmatrix}$ is applied to the sample, the dislocations feel a force [Fig. 3(a)] and would like to move in such a way as to relax the stress. One might expect a deformation of the grain as shown in Fig. 3(b). However, for such a deformation the dislocation density is no longer the same along the boundaries of the grain, assuming that no interstitials and vacancies are emitted or absorbed by the boundary. The nonuniform dislocation density gives rise to a distortion of the crystal inside the grain. We expect a high energy for such a distorted lattice, so that the deformation shown in Fig. 3(b) is very unlikely. On the other hand, the deformation shown in Fig. 3(c) preserves the constant line density of dislocations and does not give rise to a macroscopic distortion of the grain. In this configuration the grain boundaries are effectively pinned at the corners of the grain.

We now discuss how such a metastable configuration can actually be relaxed by dislocation climb and estimate its lifetime. If dislocations are allowed to climb, the grain can shrink, thereby increasing the angle of the grain with respect to the lattice outside. To avoid distortions of the crystal inside, the dislocation spacing has to remain uniform during the process of shrinking (see Fig. 4). The total energy of the grain boundary decreases with d as

$$\frac{\partial E}{\partial d}=\frac{N_0 K a_0^2}{2\pi d}\ , \tag{2.26}$$

where N_0 is the number of dislocations on one side of the grain. Assuming that glide proceeds instantaneously (much faster than climb), we may make the following guess of an approximate equation of motion for the displacement $\eta_i(t)$ of the dislocations perpendicular to their Burgers vectors (climb):

$$\gamma_{\mathrm{GB}}\dot{\eta}_i(t)=-\frac{\partial}{\partial\eta_i}E\{\eta_i\} \tag{2.27}$$

Here γ_{GB} is a phenomenological friction coefficient

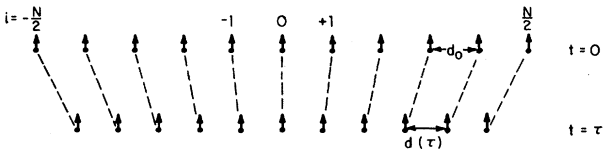

FIG. 4. Positions of the dislocations on one side of a square grain when climb is allowed. At $t=0$, the dislocation separation is d_0; at $t=\tau$, it is $d(\tau)$. The central dislocation does not climb.

for climb of dislocations in the grain boundary. We shall see that γ_{GB} itself depends sensitively on the geometry of the system.

For the uniform contraction of the grain boundary, which is under consideration, we have

$$\eta_j(t)=j[d(t)-d_0]\ . \tag{2.28}$$

Assuming the validity of Eq. (2.27), we can find the rate of change of $d(t)$ by summing over the dislocations of half a grain boundary,

$$\sum_{i=1}^{N/2}\gamma_{GB}\dot{\eta}_i=\sum_{i=1}^{N/2}\gamma_{GB}i\dot{d}(t)\simeq\gamma_{GB}\frac{1}{2}\left[\frac{N}{2}\right]^2\dot{d}(t)\ ,$$
$$=-\sum_{i=1}^{N/2}\frac{\partial}{\partial\eta_i}E\{\eta_j\}=-\frac{1}{8}\frac{\partial E}{\partial d}\ , \tag{2.29}$$

and argue that the sum in (2.29) should be equal to $\frac{1}{8}$ of the total change in energy with dislocation spacing d. The resulting equation of motion for $d(t)$ is

$$\dot{d}=-\frac{Ka_0^2D_\perp^{GB}}{2\pi N_0 d^2 k_B T}d\ , \tag{2.30a}$$

$$D_\perp^{GB}\equiv k_BT/\gamma_{GB}\ , \tag{2.30b}$$

where $D_\perp^{GB}$ has the dimensions of a diffusion constant. This gives us the result for the decay time of the grain boundary

$$\tau\sim\frac{N_0d^2}{D_\perp^{GB}}\ . \tag{2.31}$$

So far we have not taken into account the deviation of defects from their equilibrium concentration. As a dislocation climbs it must emit or absorb vacancies or interstitials. If it emits vacancies the local vacancy concentration is increased above its equilibrium concentration, creating a gradient in the vacancy chemical potential which then gives rise to a vacancy current. If a grain boundary climbs as a whole, many vacancies are simultaneously absorbed (or emitted). For the process to continue, more vacancies have to diffuse to (away from) the grain boundary. We therefore expect the diffusion of a grain boundary with many dislocations to be considerably delayed as compared to the climb of a single dislocation.

To find the appropriate diffusion constant for climb motion of dislocations in a grain boundary, we will use a method similar to Mott's[17] for grain boundaries in three-dimensional crystals. We consider a simple situation in which two parallel grain boundaries with opposite Burgers vectors are climbing with the same average velocity $\langle v\rangle$ (Fig. 5). This kind of motion is only possible in an inhomogeneous stress field. For simplicity we take a stress $\sigma_{22}(+D/2)=-\sigma_{22}(-D/2)$, which may arise from an "external force" applied to the midline between the grain boundaries. The top row then acts as a sink and the bottom row as a source of vacancies (the other way around for interstitials). For the climb motion to continue, defects have to diffuse from the sources to the sinks, i.e., across the distance D from one grain boundary to the other. This process reduces climb motion of a grain boundary as we will show now. We use here the equations of motion derived in Ref. 7.

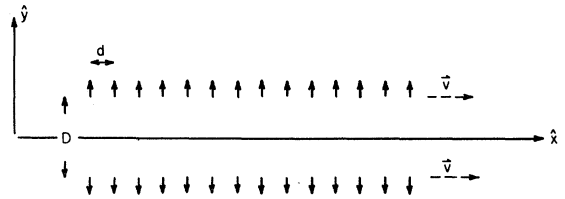

FIG. 5. Two grain boundaries along $\hat{x}$ with opposite Burgers vectors along $+y$ and $-y$ are climbing along x with the same velocity v. Vacancies are moving along $\hat{y}$ from sources (at $y=D/s$) to sinks (at $y=-D/2$).

Following Ref. 7, we define a defect density as the difference between the density of interstitials and vacancies:

$$n_\Delta=n_I-n_V\ . \tag{2.32}$$

Then the equation of motion for the dislocations on the two rows at $\pm D/2$ is

$$\langle v\rangle(\pm D/2)=\pm\frac{a_0D_\perp}{k_BT}\left[2\sigma_{22}(\pm D/2)+\frac{\delta n_\Delta(\pm D/2)}{n_0\chi}\right]\ , \tag{2.33}$$

where n_0 is the number density of atoms and $\delta n_\Delta=n_\Delta-n_\Delta^0$ is the deviation of the defect density from its equilibrium value n_Δ^0, which we assume to be small. The inverse susceptibility χ^{-1} measures the increase in free energy per unit area due to a change in the defect concentration[7]:

$$\delta F=\tfrac{1}{2}\chi^{-1}\int d^2r(\delta n_\Delta/n_0)^2\ . \tag{2.34a}$$

Treating the defects as an ideal gas, one finds

$$\chi^{-1}\sim\frac{n_0^2 k_B T}{n_\Delta^0}\ , \tag{2.34b}$$

which becomes very large for low temperatures.

The constant $D_\perp$ in (2.33) is the diffusion constant for climb of a free dislocation under conditions where the local concentrations of interstitials and vacancies are maintained at their thermal equilibrium values, through the influence of some nearby source or sink. (The diffusion constant $D_\perp$ should be smaller than the glide constant $D_{||}$ roughly in proportion to the equilibrium concentration of defects, which leads us to our estimate $D_\perp\approx 10^{-10}$ cm^2/sec.) In the present situation of two climbing grain boundaries, no local sources for defects are present, and the defects have to diffuse from one boundary to the other according to the equation of motion[7]

$$\partial_t\delta n_\Delta = D_\Delta\nabla^2\delta n_\Delta - \frac{\langle v\rangle}{a_0}\sum_\nu \delta(\vec{r}-\vec{r}_\nu)b_\nu^y\ . \tag{2.35}$$

The defect diffusion constant is denoted by D_Δ and the summation runs over all dislocations with $b_\nu^y=\pm 1$. The steady state solution of Eq. (2.35) is

$$\delta n_\Delta(\vec{r})=\frac{1}{4\pi a_0}\frac{\langle v\rangle}{D_\Delta} \times\sum_\nu \ln\left|\frac{(y-D/2)^2+(x-\nu d)^2}{(y+D/2)^2+(x-\nu d)^2}\right|\ . \tag{2.36}$$

At the positions of the dislocations, the excess defect concentration is then

$$\delta n_\Delta\left[\pm\frac{D}{2}\right]=\mp\frac{1}{2\pi a_0}\frac{\langle v\rangle}{D_\Delta}\left\{\ln\frac{D}{a_0}+\ln\left[\sinh\left[\frac{\pi D}{d}\right]\right] -\ln\left[\frac{\pi D}{d}\right]\right\}, \tag{2.37}$$

where we have cut off the divergent logarithm at the lattice constant. If this expression is substituted into Eq. (2.33) we find for the velocity of the dislocations in the stress field σ in the limit $D>>d$:

$$\langle v\rangle\left[\pm\frac{D}{2}\right]\left[1+\frac{D_\perp}{D_\Delta}\frac{n_0\chi^{-1}}{k_B T 2\pi}\left[\ln\frac{d}{a_0\pi}+\pi\frac{D}{d}\right]\right] =2\frac{a_0 D_\perp}{k_B T}\sigma_{22}\ . \tag{2.38}$$

The climb diffusion constant $D_\perp$ of a single dislocation is roughly given by the vacancy diffusion constant D_Δ times the defect concentration n_Δ^0/n_0. Using, furthermore, the estimate (2.34) for χ we find in the limit $D>>d$

$$\langle v\rangle\approx\frac{d a_0 D_\perp}{D k_B T}\sigma\ . \tag{2.39}$$

Comparing this result with the phenomenological expressions (2.27) and (2.30b) we find

$$D_\perp^{\mathrm{GB}}\approx D_\perp\frac{d}{D}\ . \tag{2.40}$$

So far we have looked at a very special geometry of grain boundaries. In a more general situation we expect a similar reduction of $D_\perp^{\mathrm{GB}}$, which is determined by the ratio of the dislocation spacing within one grain boundary to the distance between defect sources and sinks. For example, for the uniform shrinkage of a grain, as discussed above, the distance D is of the order of the length of one grain boundary L. The decay time (2.31) can then be estimated as

$$\tau\sim\frac{L^2}{D_\perp}\ . \tag{2.41}$$

For the grain to be stable over a period of 10^3 sec, we have to require $L\gtrsim 10^{-2}$ cm.

D. Dislocation pairs of large separation

In a solid in equilibrium only tightly bound dislocation pairs are present. These pairs can reduce the elastic constants only slightly. Also, the energy dissipation in an applied, low-frequency shear will be small, since the diffusive motion of such small pairs is rapid with a characteristic frequency $\omega\sim D_{||}/r^2$, where r is the separation of the pair.

We now consider a situation, where some dislocation pairs of large separation have been frozen in. If these pairs can relax to their equilibrium separation only by climb motion, they can be considered metastable in a system of low defect concentration.

The interaction energy of a dislocation pair, separated a distance r is

$$E(\theta)=\frac{K a_0^2}{4\pi}\left[\ln\frac{r}{a_0}-\cos^2\theta\right], \tag{2.42}$$

where θ denotes the angle between $\vec{r}$ and $\vec{b}$. For

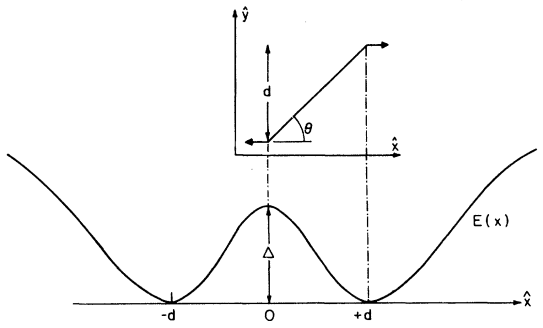

FIG. 6. Interaction energy $E(x)$ of a neutral pair of dislocations is shown as a function of the separation along the glide direction $\hat{x}$. Their separation d in the climb direction $\hat{y}$ is assumed constant.

fixed $r_\perp = d$, this energy has two minima for $\cos^2\theta = \frac{1}{2}$, corresponding to the two configurations shown in Fig. 6. The two configurations have the same energy and are separated by an energy barrier of height.

$$\Delta E_0 = E(\theta=0) - E(\theta=45°) = \frac{Ka_0^2}{4\pi}(1-\ln 2) . \tag{2.43}$$

In an activated process the system can flip back and forth between the two minima. We write the hopping rate W

$$W = \nu_0 e^{-\Delta E_0/k_B T} , \tag{2.44}$$

as the product of a Boltzmann factor and a microscopic attempt frequency ν_0. For a single layer film, if the elastic constant K is near the Kosterlitz-Thouless lower bound,[5] $Ka_0^2 = 16\pi k_B T$, the energy barrier is $\sim 0.6 k_B T$.

The interaction energy of the pair with an applied shear $\sigma = \begin{pmatrix} 0 & \sigma \\ \sigma & 0 \end{pmatrix}$ is

$$\Delta E = \tfrac{1}{2}(b_k \epsilon_{ji} R_i + b_j \epsilon_{ki} R_i)\sigma_{kj} \equiv P_{kj}\delta_{kj} , \tag{2.45}$$

where we have defined a "polarization" P_{kj}. The two minima of $E(x)$ are no longer degenerate, since

$$E(x=-d) - E(x=+d) = 2d\tilde{\sigma} = 2d\sigma(b_x^2 - b_y^2) , \tag{2.46}$$

and consequently the density of pairs n_1 with energy $E(x=-d)$ is reduced in favor of n_2, the density of pairs with energy $E(x=d)$:

$$\frac{n_1}{n_2} = e^{-2d\tilde{\sigma}/k_B T} \simeq 1 - 2d\tilde{\sigma}/k_B T . \tag{2.47}$$

This difference in occupation number gives rise to a polarization. Following Ref. 7 we introduce a generalized dynamic susceptibility χ^0 and find

$$\begin{aligned} P_{xy} &= \chi^0_{xyxy}\sigma_{xy} \\ &= -\tfrac{1}{2} b_x^2 d(n_1 - n_2) \\ &= -\tfrac{1}{2} b_x^2 n_0(d) d^2 \frac{\sigma}{k_B T}(b_x^2 - b_y^2) , \end{aligned} \tag{2.48}$$

where $n_0(d)$ denotes the total number of pairs with $r_\perp = d$. Averaging over Burgers vectors and integrating over space we find the static susceptibility

$$\chi^0 = \chi^0_{xyxy} = \frac{\pi}{2k_B T}\int_{a_0}^{\infty} ds\, s^3 n_0(s) . \tag{2.49}$$

If the stress is switched off at $t = t_0$, the polarization will relax to zero at a rate W:

$$(n_1 - n_2)(t) = (n_1 - n_2)(t_0) e^{-2W(t-t_0)}, \quad t \geq t_0 . \tag{2.50}$$

Thus the dynamic susceptibility is

$$\chi_{xyxy}(\omega) = \frac{\pi}{2k_B T}\int_{a_0}^{\infty} ds\, s^3 \frac{2W}{-i\omega + 2W} n_0(s) . \tag{2.51}$$

The activation energy is of the order of $k_B T$,

$$\frac{\Delta E_0}{k_B T} \simeq 4(1-\ln 2) \sim 0.6 , \tag{2.52}$$

and the attempt frequency can be estimated as

$$\nu_0 \sim \frac{D_{\parallel}}{r^2} , \tag{2.53}$$

If we allow for pairs with separation r up to 10^4 Å, the relaxation times can be as long as 10^{-2} sec. In a system which is not truly 2D but consists of several layers, we expect the activation energy to increase with increasing film thickness, so that the relaxation can be considerably delayed. If the interactions between dislocations of different pairs are taken into account, one finds a distribution of local minima, separated by barrier heights, which depend continuously on the various separations.

The relaxation of the pair to equilibrium requires climb motion of the two dislocations. The corresponding lifetime can be estimated as

$$\tau \sim \frac{r^2}{D_\perp} \sim 100 \text{ sec} . \tag{2.54}$$

for the values of the parameters as chosen above.

III. LARGE-ANGLE GRAIN BOUNDARY

So far we restricted ourselves to low-angle grain boundaries. If the separation between dislocations becomes comparable to the lattice spacing, then one cannot distinguish the dislocations and a different picture must be used. The region near a high-angle grain boundary is highly strained, and close to T_c, it may be appropriate to treat the grain boundary as a thin line of liquid, allowing no tangential shear stress in the absence of motion. When shear stress is applied to the macroscopic sample, there will be a relaxation due to slippage at the grain boundaries which will lead to a decrease in the measured dc shear modulus.

The renormalization of the shear modulus has been studied numerically by Gharemani[24] for a regular hexagonal array of crystallites (Fig. 7). Gharemani's results may be fitted by the equation[25]

$$\frac{\mu_R}{\mu}=\frac{(0.86+0.03\nu_2)(1+2\nu_2)}{(1.14+1.97\nu_2)} , \tag{3.1}$$

where μ_R is the renormalized two-dimensional shear modulus and ν_2 is the two-dimensional Poisson ratio of the constituent grains, related to the unrenormalized 2D Lamé coefficients by

$$\nu_2=\lambda/(2\mu+\lambda) . \tag{3.2}$$

Formula (3.1) predicts a 14% renormalization of the shear modulus for an incompressible system ($\nu_2=1$) and slightly larger renormalizations for smaller values of ν_2. Somewhat larger renormalizations may be obtained for other geometries of grain boundaries,[26] but it seems unlikely that this mechanism could lead to reductions as large as 50%.

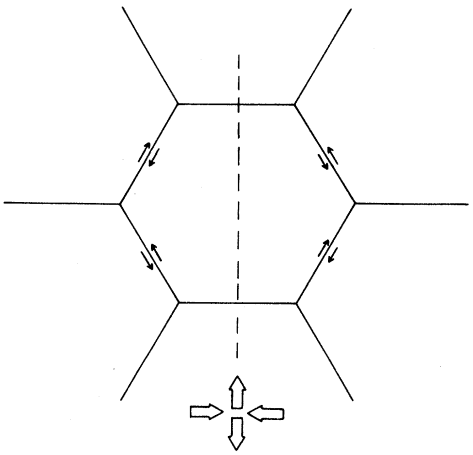

FIG. 7. Hexagonal network of high-angle grain boundaries. The arrows indicate slipping along the liquidlike boundaries under a tensile stress indicated by the fat arrows.

The time necessary for the completion of the renormalization of μ is the time necessary for complete relaxation of the tangential stress σ across the boundary of two neighboring grains under a given constant shear strain U_{xy} across the boundary. Let s be the amount of slippage of two grains separated by a liquid band of width w and three-dimensional viscosity η. Then, using the definition of η we find

$$h\eta\frac{\dot{s}}{w}=\sigma , \tag{3.3}$$

where h is the film thickness. If u_{xy} is the shear strain *within* each grain, then

$$\sigma=2\mu u_{xy} , \tag{3.4}$$

where μ is the two-dimensional shear coefficient. The total shear strain across the two grains is

$$U_{xy}=u_{xy}+s/L , \tag{3.5}$$

where L is the grain size. Eliminating u_{xy} and σ we find

$$h\eta\frac{\dot{s}}{w}=2\mu(U_{xy}-s/L) . \tag{3.6}$$

The characteristic time τ for the stress to relax is

$$\tau=\eta Lh/\mu w . \tag{3.7}$$

Choosing the parameters as $L\approx 1$ mm, $\eta\approx 0.1$ poise (typical for nematics), $h=30$ Å (monolayer of smectic), and $w=5$ Å, one finds $\tau\approx 10^{-3}$ sec, if μ is given by the Kosterlitz-Thouless value (~ 220 erg/cm^2).

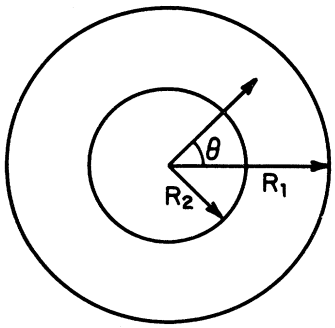

FIG. 8. Schematic geometry of the experiment of Sprenger *et al.* (Ref. 6). The smectic-*B* film fills the annulus between R_2 and R_1, with $R_2-R_1<<R_1$. The central disk is attached to a torsion fiber. The aximuthal angle is θ.

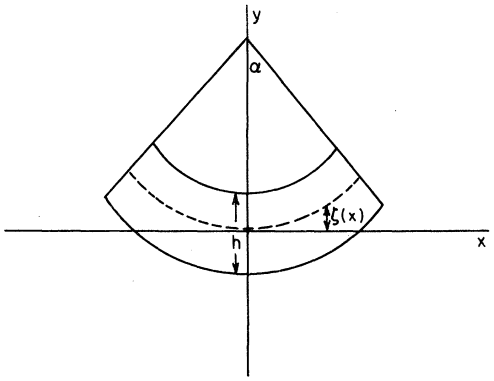

FIG. 9. Bent section of an initially straight crystal. The crystal of width ΔR is bent over α radians. The neutral surface, where the crystal is not deformed, is indicated by $\zeta(x)$.

IV. DEFECTS IN A BENT CRYSTAL

In the recent experiments by Sprenger *et al.*,[6] the shear coefficient of a free-standing smectic-*B* film is measured with a disk of radius R_1 attached to a torsion fiber (Fig. 8). The smectic-*B* film is in the annulus between R_1 and R_2. If we suppose that the interaction between the smectic film and the boundary is such as to orient the crystal axes in a particular way with respect to the boundary, then the crystal may be forced to contain dislocations or grain boundaries even in its equilibrium state. This occurs because if defects were not present, the boundary conditions would require that the crystal be bent into an annulus, with a high cost of elastic energy.

The elastic energy of the crystal without defects can, for this geometry, be found as follows[27]: Let $\zeta(x)$ describe the neutral surface of the bent crystal (Fig. 9). At the neutral surface there is no compression or shear. From Fig. 9 we see that

$$\zeta(x)\simeq\frac{1}{2}\frac{x^2}{R}\ , \tag{4.1}$$

with $R=\frac{1}{2}(R_1+R_2)$. If no forces are applied at the surface, then the stress tensor σ_{ik} has to fulfill the boundary condition

$$n_k\sigma_{ik}=0\ , \tag{4.2}$$

where $\vec{n}$ is the normal to the surface. In the limit $R_1\to R_2$ this implies

$$\sigma_{iy}\simeq 0 \tag{4.3}$$

also inside the material. Equation (4.3) can be used to determine the components of the strain field:

$$u_{xy}\simeq 0\ , \tag{4.4}$$

$$u_{xx}+\frac{2\mu+\lambda}{\lambda}u_{yy}\simeq 0\ . \tag{4.5}$$

On the other hand, we know that to lowest order in $\zeta(x)$,

$$\partial_x u_y=\partial_x\zeta(x)\ , \tag{4.6}$$

and therefore, since $(\partial_x u_y+\partial_y u_x)=2u_{xy}=0$,

$$\partial_y u_x=-\partial_x\zeta(x)\ . \tag{4.7}$$

Integrating (4.7) one finds

$$u_x\simeq -y\partial_x\zeta(x)\ , \tag{4.8}$$

$$u_{xx}\simeq -y\frac{\partial^2}{\partial x^2}\zeta(x)\ , \tag{4.9}$$

and with the help of (4.5),

$$u_{yy}\simeq\frac{\lambda}{2\mu+\lambda}y\frac{\partial^2}{\partial x^2}\zeta(x)\ . \tag{4.10}$$

It is now straightforward to calculate the elastic energy E:

$$E=\int d^2r\left[\mu u_{ij}u_{ij}+\tfrac{1}{2}\lambda(u_{kk})^2\right]\ , \tag{4.11}$$

since we know $\zeta(x)$ [Eq. (4.1)]. The result is

$$E=\frac{2}{3R}\left[\frac{\Delta R}{2}\right]^3\left\{\mu\left[1+\left[\frac{\lambda}{2\mu+\lambda}\right]^2\right]+\frac{\lambda}{2}\left[\frac{2\mu}{2\mu+\lambda}\right]^2\right\}2\alpha, \tag{4.12}$$

where $\Delta R=R_2-R_1$, 2α is the angle spanned by

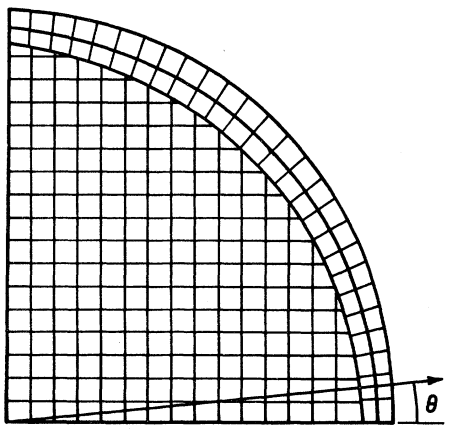

FIG. 10. A high-angle surface grain boundary for a circular crystal with square symmetry. The misfit angle between crystal axes is θ.

the bent segment of material (see Fig. 9), and we have assumed $\Delta R << R$.

We now discuss possible ways to reduce the elastic free energy (4.12) by introducing defects into the solid. One example is a high-angle grain boundary along the edges of the sample, such that the boundary condition on the crystal axis is satisfied. Then the crystal can be unstrained except for a narrow region along the boundary.

For simplicity we choose a crystal with square symmetry. The misfit angle of the grain boundary θ is then just the azimuthal angle (Fig. 10). The energy ϵ per unit length of grain boundary is [Eq. (2.3)]

$$\epsilon=\frac{E_c}{d}+\frac{Ka_0^2}{8\pi d}\ln(d/2\pi a_0)$$
$$=\theta\left[\frac{E_c}{a_0}-\frac{Ka_0}{8\pi}\ln(2\pi\theta)\right], \tag{4.13}$$

where d is the separation between dislocations and $\theta=a_0/d$. This formula is of course only valid for small θ. To get a rough estimate we will use it for $0<\theta<\pi/4$. The total energy of the grain boundary at R_1 is

$$E_1=8R_1\int_0^{\pi/4}d\theta\,\theta\left[\frac{E_c}{a_0}-\frac{Ka_0}{8\pi}\ln(2\pi\theta)\right] \tag{4.14}$$

$$=\tfrac{1}{4}\pi^2R_1\left[\frac{E_c}{a_0}-\frac{Ka_0}{4\pi}(\ln\pi-\tfrac{1}{2}\ln 2-\tfrac{1}{4})\right], \tag{4.15}$$

and a similar expression for the grain boundary at R_2. Comparing this with Eq. (4.12) we find that the energy is indeed reduced if

$$R^2a_0<(\Delta R)^3 . \tag{4.16}$$

For the experimental geometry, $R\simeq 1$ cm and $\Delta R\simeq 1$ mm while $a_0\sim 5$ Å and the inequality is well satisfied.

If, in three dimensions, a crystal is bent, then one finds a third possibility called polygonization.[28] The crystal consists of polygons of undeformed crystal, separated by low-angle *radial* grain boundaries (Fig. 11). Let $\theta=a_0/d$ be the misfit angle. If the crystal is bent in a circle, then there are N_g grain boundaries with

$$N_g\theta=2\pi . \tag{4.17}$$

Each grain boundary contains $\Delta R/d$ dislocations

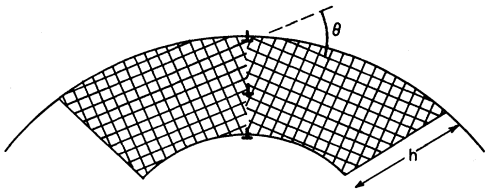

FIG. 11. Example of polygonization in a bent crystal. The radial grain boundaries relax the strain energy of the bent crystal in Fig. 9. The Burgers vectors of the dislocations are tangential.

(see Fig. 11). The total number of dislocations N_D is

$$N_D=2\pi\Delta R/a_0 . \tag{4.18}$$

The density n of dislocations is

$$n=2\pi\Delta R/[(a_0\pi(R_2^2-R_1^2)]\simeq 1/Ra_0 . \tag{4.19}$$

Using Eq. (4.13), one finds that the total energy E

$$E=N_g\epsilon\Delta R=\frac{2\pi}{a_0}\Delta R\left[E_c-\frac{Ka_0^2}{8\pi}\ln(2\pi\theta)\right] \tag{4.20}$$

is proportional to ΔR, the width of the annulus. Therefore, if $\Delta R<R$, as in the experiment of Sprenger *et al.*,[6] it is energetically more favorable to introduce radial, small-angle grain boundaries than large-angle grain boundaries along the edge of the rim.

Actually, there is still some mismatch at the surface. The surface misfit angle varies between $+\theta/2$ to $-\theta/2$ in one polygon. The surface energy for one polygon, E_s^1, at $R=R_1$ is

$$E_s^1=R_1\int_{-\theta/2}^{\theta/2}d\theta'\epsilon(\theta') , \tag{4.21}$$

and the total surface energy E_s is

$$E_s=N_g(E_s^1+E_s^2) \tag{4.22a}$$

$$=\frac{\pi\theta}{2}(R_1+R_2)\left[\frac{E_c}{a_0}-\frac{Ka_0}{4\pi}(\tfrac{1}{2}\ln\pi\theta-\tfrac{1}{4})\right], \tag{4.22b}$$

and is a factor $\theta R/\Delta R$ smaller than E. The actual value of θ is found by minimizing $E+E_s$. If $E_c\gtrsim Ka_0^2$, one finds

$$\theta=\simeq\frac{1}{4\pi}\frac{\Delta R}{R}\frac{Ka_0^2}{E_c} , \tag{4.23}$$

which is indeed small.

V. MOTION OF FREE DISLOCATIONS

In this section we discuss the simplest configuration of dislocations which can give rise to an effective viscosity and apply it to the experiment of Sprenger *et al.*[6] Let us consider an array of dislocations distributed over the sample with density n. If this array is caused by polygonization, as discussed in the preceding section, then all Burgers vectors are tangential, and $n \sim 1/Ra_0$ with R the mean radius in Fig. 8:

$$R = \tfrac{1}{2}(R_1 + R_2) . \tag{5.1}$$

In this case, dislocations can glide without changing their separation from each other. If a constant shear stress σ is applied, then dislocations glide with a velocity $\langle v \rangle$ given by

$$(k_B T/D_{||})\langle v \rangle = \sigma a_0 . \tag{5.2}$$

If N dislocations have moved around a circle and come back to their original position, then the inner disc has slipped a distance Na_0. The slipping velocity $V = R\theta$ is then

$$V = n\frac{R_1^2 - R_2^2}{R} a_0 \langle v \rangle \tag{5.3}$$

(we assume here that $R_1 - R_2 << R$). Combining (5.2) and (5.3) we obtain an effective two-dimensional viscosity

$$\eta_{\text{eff}} \equiv \frac{\sigma(R_1 - R_2)}{V} = k_B T/(2a_0^2 n D_{||}) . \tag{5.4}$$

If $n \sim 1/Ra_0$, as in the preceding section, we get

$$\eta_{\text{eff}} \cong R k_B T/D_{||} a_0 .$$

If the inner disk is driven by a torsion wire with torsional constant κ, then the applied stress is not constant in time but decreases according to

$$2\pi R^2 \frac{d\sigma}{dt} = -\kappa V/R , \tag{5.5}$$

where V is the velocity of the inner disk.

The (immediate) elastic response of the film to the change in stress must now be added to the contribution (5.3) from dislocation motion, so that we find for the velocity of the sample at its inner edge

$$V = \left[\frac{1}{\mu}\frac{d\sigma}{dt} - \frac{\sigma}{\eta_{\text{eff}}}\right](R_2 - R_1) . \tag{5.6}$$

Matching the velocities in (5.5) and (5.6), we have

$$\frac{d\sigma}{dt} = \frac{-\sigma\mu}{\eta_{\text{eff}}}\left[1 + \frac{2\pi\mu R^3}{\kappa(R_1 - R_2)}\right]^{-1} . \tag{5.7}$$

In the limit of large torsion constant κ, one obtains the stress relaxation rate μ/η_{eff} applicable to a sample with constant strain. If η_{eff} is given by (5.4), and if we assume $D_{||} \approx 10^{-6}$ cm^2/sec, $a_0 \approx 5$ Å, $R \approx 1$ cm, and $\mu \approx 220$ erg/cm^2 (the Kosterlitz-Thouless value for one layer), then we find $\eta_{\text{eff}}/\mu \approx 0.01$ sec.

VI. FLOW AT A BOUNDARY

Interesting effects can occur if there is a narrow liquid band at a junction of the sample and the containing walls. A liquid band may well occur, at temperatures near the melting temperature, because of strains on the atomic scale, arising from the mismatch between the crystal structures of the sample and the wall.

If the sample boundary is smooth on the macroscopic scale, and perfectly circular, then slip between the sample and boundary can occur rather easily, and one would find a characteristic relaxation time of the order of that given by Eq. (3.7). If the surface is rough, however (say of the scale of 1 μm), then slip is a much slower process which requires melting the sample at some points of the boundary, flow through the liquid band, and recrystallization at other points on the boundary.[29]

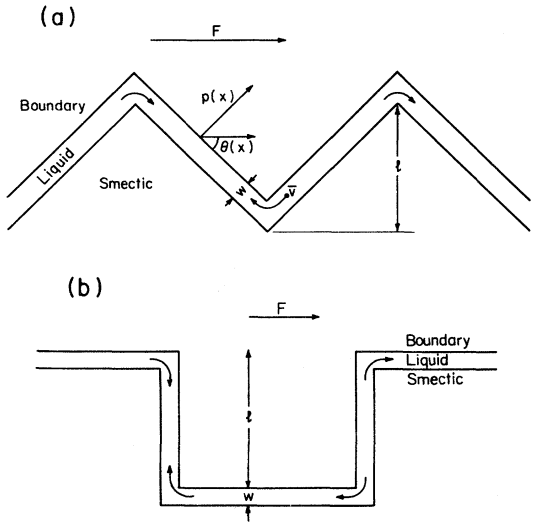

FIG. 12. Boundary between smectic and container. The width of the liquid band is w, the height of the surface irregularities is l, and the angle of the surface with the average surface is θ.

This process can be illustrated for some simple geometries, such as those shown in Fig. 12. Let $\theta(x)$ be the local angle of the surface with the average direction of the surface and assume that a force F has been applied to the boundary (see Fig. 12). We want to calculate the velocity V with which the smectic slips along the boundary. The force will push the smectic against the boundary and induce a pressure $p(x)$ in the liquid layer. The applied force obeys

$$F=h\oint dx\, p(x)\sin\theta(x)\ , \tag{6.1}$$

where h is the film thickness and the integral extends over the boundary. The pressure will create a flow as indicated in Fig. 12. Let $\bar{v}(x)$ be the average flow velocity at x. For Poisseuille flow

$$\bar{v}(x)=-\frac{1}{12\eta}w^2\cos\theta(x)\frac{dp(x)}{dx}\ , \tag{6.2}$$

where w is the width of the liquid band and η is the three-dimensional viscosity of the liquid. If the width is to remain constant then the mass flow has to be compensated by the dissolving of solid into liquid in some places and solidification in other places. The volume $d\Omega$ of liquid leaving the band between x and $x+\Delta x$ per unit time is

$$\frac{d\Omega}{dt}=-\Delta x w h\frac{d\bar{v}(x)}{dx}\ . \tag{6.3}$$

Since the solid is moving with a velocity V, an amount $d\Omega'$ of solid is dissolving per unit time:

$$\frac{d\Omega'}{dt}=\Delta x V h\sin\theta(x)/\cos\theta(x)\ . \tag{6.4}$$

In equilibrium, $d\Omega=d\Omega'$, so

$$V=\frac{d\bar{v}}{dx}w\cos\theta(x)/\sin\theta(x)\ . \tag{6.5}$$

Equations (6.1), (6.2), and (6.5) determine the friction constant γ:

$$F=\gamma V\ . \tag{6.6}$$

Let $\theta(x)$ be small. For the geometry of Fig. 11 one can define the surface by the distance $R(x)$ from the center, where x measures the distance along the perimeter of the circle with radius $\langle R\rangle$. For small θ, $R(x)$ is related to $\theta(x)$ by

$$\theta(x)=\frac{d}{dx}R(x)\ . \tag{6.7}$$

The friction coefficient is then

$$\gamma=\frac{12\eta h(2\pi\langle R\rangle)}{w^3}(\langle R^2\rangle-\langle R\rangle^2)\ . \tag{6.8}$$

If $\theta(x)$ is large, then Eq. (6.8) does not hold. For the geometry of Figs. 12(a) and 12(b) one finds

$$\gamma=\frac{\eta h}{w^3}L_s l^2 \tag{6.9a}$$

and

$$\gamma=\frac{12\eta h}{w^3}L_s l^2\ , \tag{6.9b}$$

respectively, where L_s is the length of the boundary and l the height of the surface irregularity, as indicated in the figures. The slipping along the boundary gives an effective two-dimensional viscosity $\eta_{\rm eff}$ for the film, which is related to γ by

$$\eta_{\rm eff}=\gamma(R_2-R_1)/2\pi R_1\ . \tag{6.10}$$

If l or $(\langle R^2\rangle-\langle R\rangle^2)^{1/2}$ is of the order of 1 μm, $\eta\approx 0.1$ poise, $w\approx 5$ Å, and $h\approx 30$ Å (monolayer of smectic), then one finds $\eta_{\rm eff}\approx 10^6$ poise cm. The characteristic time $\tau=\eta_{\rm eff}/\mu$ becomes very long ($\sim 10^4$ sec) using the Kosterlitz-Thouless value for μ. To get relaxation times of the order of seconds one needs very smooth, precisely circular boundaries:

$$(\langle R^2\rangle-\langle R\rangle^2)^{1/2}\lesssim 100\ \text{Å}\ . \tag{6.11}$$

VII. NONLINEAR EFFECTS

A. Dissociation of pairs

In the presence of a finite stress field σ, free dislocations can be nucleated from pairs.[30] For simplicity we consider a square lattice and look for a stationary solution of the Fokker-Planck equation for the density of pairs $\Gamma^\alpha(\vec{r})$ with Burgers vector $\vec{b}^\alpha$ and separation $\vec{r}$,[7]

$$\frac{\partial\Gamma^\alpha}{\partial t}=-\partial_i j_i^\alpha\ , \tag{7.1a}$$

$$j_i^\alpha=-2D_{ij}^\alpha e^{-u}\partial_j(e^u\Gamma^\alpha)\ , \tag{7.1b}$$

with the potential $U(\vec{r})=u(\vec{r})k_BT$,

$$U(\vec{r})=U_0(\vec{r})+\frac{a_0}{2}(b_k\epsilon_{ji}r_i+b_j\epsilon_{ki}r_i)\sigma_{jk}\ , \tag{7.2a}$$

and

$$U_0(\vec{r})=\frac{Ka_0^2}{4\pi}\left[\ln\frac{r}{a_0}-\frac{(\vec{b}^\alpha\cdot\vec{r})^2}{r^2}\right]-2E_c\ . \tag{7.2b}$$

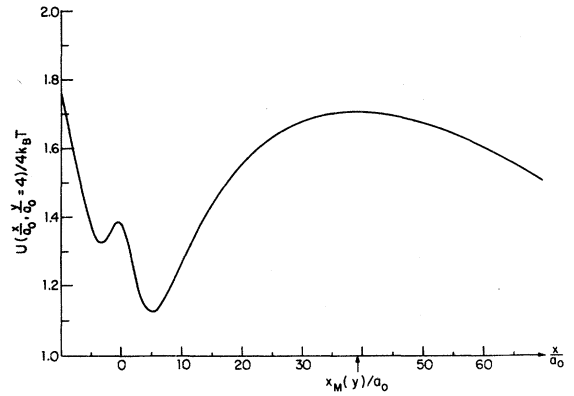

FIG. 13. Potential $U(x,y)$ of a dislocation pair in an applied stress field as a function of x, the pair separation in the glide direction. The position of the maximum $x_M(y)$ depends on the pair separation in the climb direction, which has been chosen as $y=4a_0$.

It is convenient to work in the coordinate system in which the Burgers vector under consideration points along the x axis. The applied shear then has the components

$$\tilde{\sigma}=\sigma\begin{bmatrix}\sin 2\theta & \cos 2\theta\\ \cos 2\theta & -\sin 2\theta\end{bmatrix}, \tag{7.3}$$

where θ denotes the angle between the axis of applied shear σ and the $\hat{x}$ direction.

In the case of a highly anisotropic diffusion tensor $D_\perp << D_{||}$, the dislocation motion is approximately one dimensional. The current is purely in the x direction and the Fokker-Planck equation (7.1) holds separately for all pairs with a fixed separation in the y direction:

$$\partial_t \Gamma^\alpha(x,y)=-\partial_x j_x^\alpha(x,y). \tag{7.4a}$$

A stationary solution of (7.4a) requires

$$j_x^\alpha(x,y)=j(y)\ . \tag{7.4b}$$

A dislocation gliding along the x direction with fixed y feels a force $F(x)=-\partial U(x,y)/\partial x$. Since the stress component $\tilde{\sigma}_{xx}$ leads only to a constant force in the climb direction, it is convenient to ignore it and use instead of (7.2a),

$$U(\vec{r})=U_0(\vec{r})-a_0 x\tilde{\sigma}_{xy}\ . \tag{7.5}$$

The potential as a function of x is shown in Fig. 13. In the absence of an applied shear, the potential has two degenerate minima, as discussed in Sec. II D. If a shear is applied, the degeneracy is lifted, and more importantly, the potential goes through a maximum at $x=x_M(y)$. Under stationary conditions the Fokker-Planck equation predicts a current $j(y)$ which satisfies

$$j(y)\int_{x_0}^{\infty} dx\, e^u=-2D_{||}\int_{x_0}^{\infty} dx\,\partial_x(e^u\Gamma)\ . \tag{7.6}$$

The main contribution to the integral on the left-hand side comes from the region $x\sim x_M(y)$. Expanding the potential around the maximum we find

$$\int_{x_0}^{\infty} e^u dx = e^{u(x_M,y)}\left[2\pi\Big/\left|\frac{\partial^2 u(x_M,y)}{\partial x^2}\right|\right]^{1/2}, \tag{7.7}$$

where we have assumed $x_0 << x_M(y)$. In this range of x the distribution function is given by

$$\Gamma(x,y)=N(y)e^{-[u(x,y)-u(0,y)]}\ . \tag{7.8}$$

The normalization $N(y)$ can be obtained by requiring that the total number of dislocations with the specified y should remain unchanged after the stress has been applied:

$$\int_{-x_M}^{x_M} dx\, N(y)e^{-[u(x,y)-u(0,y)]} = \int_{-\infty}^{+\infty}\Gamma_0 e^{-u_0(x,y)}dx\ , \tag{7.9}$$

which yields

$$j(y)=-2D_{||}\Gamma_0\left[\left|\frac{\partial^2 u(x_M,y)}{\partial x^2}\right|\Big/2\pi\right]^{1/2} \times e^{-u(x_M(y),y)}\,\mathrm{sech}\left[\frac{a_0\sigma y}{k_B T}\right], \tag{7.10}$$

where $\Gamma_0=1/a_0^4$. To find the total number of dislocations R escaping per unit time and film area, we integrate the current over all y. The main contribution arises from small values of y, so that we can expand around $y\sim 0$,

$$u(x_M(y),y)=u(x_c,0)+\tfrac{1}{2}\bar{K}\frac{y^2}{x_c^2}\ , \tag{7.11}$$

with

$$x_c=x_M(y=0)=\frac{Ka_0}{4\pi\sigma\cos 2\theta} \tag{7.12a}$$

and

$$\bar{K}=\frac{Ka_0^2}{4\pi k_B T}\ . \tag{7.12b}$$

Our final result is

$$R = \text{const} \times D_{||} \Gamma_0 \left[\frac{\sigma a_0^2}{k_B T} \right]^{\bar{K}} e^{-2E_c/k_B T} , \quad (7.13)$$

where the constant is of the order of 0.5. The approximations used to arrive at (7.13) are only correct if the escape over the barrier is a rare event, i.e., the barrier height large compared to $k_B T$. In our problem $\bar{K} \geq 4$, so that the condition is at least approximately valid.

So far we have neglected screening effects due to other dislocation pairs. These can be taken into account approximately by replacing $\bar{K}$ by a length-dependent function $\bar{K}(l = \ln(r/a_0))$ in (7.9). Following Ref. 30 we introduce a correlation length $\xi^-(T)$, which is supposed to diverge at T_m as

$$\xi^-(T) \sim \exp \left[\frac{c}{|T - T_m|^{\nu}} \right]$$

with c a nonuniversal constant and $\nu = 0.369 \ldots$. For $x_c >> \xi^-(T)$ we have

$$\bar{K}(l_c) = 4[1 + \tfrac{1}{4}\alpha(T)] , \quad (7.14a)$$

with

$$\alpha(T) \sim |T - T_m|^{\bar{\nu}} , \quad (7.14b)$$

and therefore

$$R \propto \sigma^{4+\alpha(T)} . \quad (7.15)$$

Neglecting the creation and annihilation of dislocations at the film edges, the rate of change of the free dislocation density n is given by

$$\frac{dn}{dt} = R - \langle v \rangle x_c n^2 . \quad (7.16)$$

The first term accounts for the nucleation of free dislocations from bound pairs and the second term approximately describes recombination. $\langle v \rangle$ is the average velocity of dislocations parallel to their Burgers vectors,

$$\langle v \rangle = \left\langle \frac{dr_{||}}{dt} \right\rangle \sim a_0 \frac{D_{||}}{k_B T} \sigma , \quad (7.17)$$

and x_c is approximately the cross section for recombination. Moving free dislocations relax a strain, as worked out in Ref. 7,

$$\partial_t w_{xy} = - \frac{D_{||} n a_0^2}{k_B T} \sigma_{xy} , \quad (7.18)$$

where $w_{xy} = \partial_x u_y$ denotes the transverse strain field. Following Ref. 30 we assume that n relaxes instantaneously to a quasi-steady-state:

$$\frac{dn}{dt} = 0, \quad n^2 = \frac{R}{\langle v \rangle x_c} . \quad (7.19)$$

From (7.18) and (7.19) it then follows that

$$\frac{\partial w_{xy}}{\partial t} \sim \sigma^{1 + \bar{K}(l_c)/2} , \quad (7.20a)$$

which for $x_c >> \xi^-$ becomes

$$\frac{\partial w_{xy}}{\partial t} \sim \sigma^{3 + \alpha(T)/2} . \quad (7.20b)$$

B. Escape of dislocations from grain boundaries

Competing with the nucleation of dislocation pairs is the escape of dislocations from a grain boundary in a finite stress field σ. As in Sec. II, we consider two pinned, parallel grain boundaries with opposite Burgers vector. The dislocations are separated by a distance d and the two grain boundaries by D and $D >> d$. Now allow each dislocation to move in its glide plane. The deviation from its equilibrium position is η. The restoring force F_x is given by [31]

$$F_x = - \frac{\partial}{\partial \eta} \left\{ \frac{K a_0^2}{4\pi} \sum_{j \neq 0} \left[-\tfrac{1}{2} \ln \left[j^2 \frac{d^2}{a_0^2} + \frac{\eta^2}{a_0^2} \right] + \frac{\eta^2}{\eta^2 + j^2 d^2} \right] \right\} \quad (7.21)$$

$$= - \frac{K a_0^2}{4\pi} \left[\frac{1}{\eta} - \frac{\pi^2 \eta}{d^2} \frac{1}{\sinh^2(\pi \eta / d)} \right] , \quad (7.22)$$

where it is assumed that only the $j = 0$ dislocation deviates from its equilibrium position. The force exerted by the second grain boundary is negligible if $D >> d$. Close to the grain boundary there is a harmonic restoring force,

$$F(x \to 0) \simeq \frac{-K a_0^2}{4} \frac{\pi x}{3 d^2} , \quad (7.23)$$

while far away

$$F(x \to \infty) \simeq \frac{-K a_0^2}{4\pi} \frac{1}{x} . \quad (7.24)$$

Thus the grain boundary acts on the escaping dislocation like another dislocation with *opposite* Burgers vector. The potential $U(x)$ can be found

by integrating the force:

$$U(x)=-\int_0^x F\,dx=\frac{Ka_0^2}{4\pi}\left\{\ln\left[\frac{\pi x}{d}\right]+\frac{\pi x}{d}\coth\left[\frac{\pi x}{d}\right]-\ln\left[\sinh\left[\frac{\pi x}{d}\right]\right]-1\right\}, \tag{7.25}$$

$$U(x\to 0)\simeq\frac{Ka_0^2}{4\pi}\frac{1}{6}(\pi x/d)^2\,, \tag{7.26}$$

$$U(x\to\infty)\simeq\frac{Ka_0^2}{4\pi}[\ln(2\pi x/d)-1]\,. \tag{7.27}$$

The dislocation is indeed confined to the grain boundary.

In an applied shear stress σ there is an additional contribution to the potential energy $\sim\sigma x$, which allows the dislocation to escape from the grain boundary. The dislocation current $j(x)$ is given as the solution of the Fokker-Planck equation:

$$\frac{\partial\Gamma(x)}{\partial t}=-\frac{\partial}{\partial x}j(x)\,, \tag{7.28}$$

$$j=-2D_{||}e^{-U(x)/k_BT}\frac{\partial}{\partial x}[e^{U(x)/k_BT}\Gamma(x)]\,, \tag{7.29}$$

Even though the presence of grain boundaries is a nonequilibrium phenomenon, we assume that in the absence of an applied shear, the distribution of dislocations in the grain boundary is given by a Boltzmann distribution

$$\Gamma(x)=C_0e^{-U(x)/k_BT}\,. \tag{7.30}$$

The constant C_0 is found by the condition

$$\int_{-\infty}^{+\infty}\Gamma(x)dx=1\,, \tag{7.31}$$

which yields at low temperatures

$$C_0^{-1}\simeq\left[\frac{6}{\pi\bar{K}}\right]^{1/2}d\,. \tag{7.32}$$

In an applied stress field more and more dislocations will escape from the grain boundary, and therefore the distribution of dislocations in the grain boundary will change with time, i.e., $\partial\Gamma(x)/\partial t$ is generally nonzero. For the moment we ignore this process, assuming that the applied stress is small. Then the analysis of Sec. VII A can be taken over. There is again a saddle point in the potential where $\partial U/\partial x=0$ given by

$$x_c=Ka_0/4\pi\sigma\,. \tag{7.33}$$

The current across the saddle point j is

$$j=\frac{2\pi}{\sqrt{3}}\frac{D_{||}}{d^2}\bar{K}e^{2\bar{K}}\left[\frac{d}{2\pi x_c}\right]^{1+\bar{K}}\,. \tag{7.34}$$

The current j is interpreted as the escape probability per unit time for one dislocation out of its potential well. Note that the potential $U(x)$ Eq. (7.27) confining a dislocation to a grain boundary is weaker than the confining potential of thermally created dislocation pairs [$U(x)=(Ka_0^2)/4\pi\ln(x/a_0)$] if $d>>a_0$ (small-angle boundary). Thus, the presence of small-angle grain boundaries may greatly enhance the production of free dislocations when an external strain is applied.

After the escape process has gone on for a while, holes will appear in the grain boundary and $\Gamma(x)$ is affected. If there is a line density $N_H(t)$ of holes then an escaping dislocation sees approximately a grain boundary with a dislocation separation $d(t)$, where

$$\frac{1}{d(t)}=\frac{1}{d}-N_H(t)\,. \tag{7.35}$$

For this approximation to hold, dislocation climb must be faster than the escape process, since the dislocations need to climb to reestablish a uniform spacing again. The approximation will break down if $N_H(t)\sim 1/d$. We simply replace now d by $d(t)$ in $\Gamma(x)$

$$\frac{d}{dt}N_H(t)=\frac{1}{d(t)}\mathscr{P}_E=\frac{1}{d(t)}j(t)\,, \tag{7.36}$$

where $\mathscr{P}_E$ represents the escape probability per unit time per dislocation. Using Eq. (7.34) with $d(t)$ instead of d we find

$$\frac{d}{dt}N_H(t)=\delta\left[\frac{1}{d}-N_H(t)\right]^{-\bar{K}+2}\,, \tag{7.37}$$

where

$$\delta=\frac{2\pi}{\sqrt{3}}D_{||}\bar{K}e^{2\bar{K}}\left[\frac{2\sigma}{Ka_0}\right]^{1+\bar{K}}\,. \tag{7.38}$$

The rate equation (7.37) is easily solved by

$$N_H(t)=\frac{1}{d}-\left[\frac{1}{d^{\bar{K}-1}}-\delta t(\bar{K}-1)\right]^{1/(\bar{K}-1)}\,. \tag{7.39}$$

If $N(t)$, the hole density, becomes comparable to $1/d$, the original dislocation density, then the grain boundary will have been annealed. The characteristic time τ_A is given by

$$\tau_A \approx 1/[\delta(\bar{K}-1)d^{\bar{K}-1}] . \tag{7.40}$$

For $\bar{K}=4$, $D_{||}=10^{-6}$ cm^2/sec, and $d=100$ Å one finds

$$\tau_A \sim (10^{-17}/U_{xy}^5) \text{ sec} , \tag{7.41}$$

where U_{xy} is the strain. To see nonlinear behavior on the time scale of the experiment we need $U_{xy} \gtrsim 10^{-4}$.

C. Sliding of grain boundaries

Finally, a third source of nonlinear effects is due to grain boundaries sliding over each other. In a sample with many different grains, one grain boundary will be intersected by others and can effectively be pinned at the intersections.

For simplicity we consider a square lattice and low-angle grain boundary intersecting another grain boundary under a 90° angle, as shown in Fig. 14. If a shear stress is applied along the vertical grain boundary, then it can glide, while the intersecting horizontal boundary remains stationary. During the glide process the vertical grain boundary feels a periodic potential of period $d_{||}$, the dislocation spacing of the intersecting boundary. The critical stress for this process is such that the gliding grain boundary can move from one minimum to the next.

The periodic potential $V(s)$ provided by the intersecting grain boundary is given by

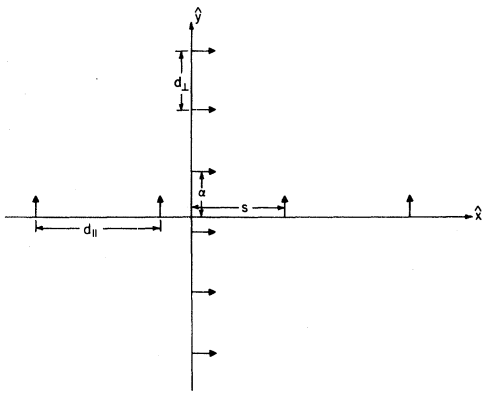

FIG. 14. A grain boundary along $\hat{y}$ is sliding over a grain-boundary along $\hat{x}$ under a shear stress along $\hat{y}$. The horizontal coordinate of the vertical boundary is given by s while $d_{||}$ and $d_\perp$ are the dislocation separations. The vertical coordinate α is assumed constant.

$$V(s)=\frac{Ka_0^2}{4\pi}\sum_{n,m}\frac{(\vec{b}_n\cdot\vec{r}_{nm})(\vec{b}_m\cdot\vec{r}_{nm})}{(\vec{r}_{nm})^2} . \tag{7.42}$$

The summation over n and m runs over all dislocations of the vertical and horizontal grain boundaries with Burgers vectors

$$\vec{b}_n=\begin{bmatrix}1\\0\end{bmatrix},\quad \vec{b}_m=\begin{bmatrix}0\\1\end{bmatrix} , \tag{7.43}$$

with dislocation spacing $d_\perp$ and $d_{||}$ and with positions

$$\vec{r}_n=(nd_\perp+\alpha)\hat{y},\quad \vec{r}_m=(md_{||}+s)\hat{x} . \tag{7.44}$$

If $d_{||} << d_\perp$, then only a few dislocations of the vertical boundary will feel the pinning potential of many dislocations of the horizontal boundary. Performing the sum over m first, we find

$$V(s,\alpha)=-\frac{Ka_0^2}{4d_{||}}\sum_n (nd_\perp+\alpha)\frac{\sin\frac{2\pi s}{d_{||}}}{\cosh\frac{2\pi}{d_{||}}(nd_\perp+\alpha)-\cos\left[\frac{2\pi}{d_{||}}s\right]} \tag{7.45}$$

The potential is periodic in s and α with period $d_{||}$ and $d_\perp$, respectively. The sum over n is effectively cut off at $n\sim d_{||}/d_\perp$, so that in the limit $d_{||} << d_\perp$ only the $n=0$ term contributes:

$$V(s,\alpha)\sim -\frac{Ka_0^2}{4d_{||}}\frac{\sin\frac{2\pi}{d_{||}}s}{\cosh\frac{2\pi}{d_{||}}\alpha-\cos\frac{2\pi}{d_{||}}s} . \tag{7.46}$$

The pinning potential has the form as shown in Fig. 15. For $\alpha\sim d_\perp$ the energy barrier decreases rapidly with increasing ratio $d_\perp/d_{||}$:

$$\Delta E \sim K a_0^2 \frac{d_\perp}{d_\parallel} e^{-\pi d_\perp / 2 d_\parallel} \quad \text{for } \alpha = d_\perp/4 \,. \tag{7.47}$$

In the opposite limit $d_\perp << d_\parallel$ many dislocations of the vertical boundary feel the pinning force of only a few dislocations of the horizontal boundary. Peforming the sum over n first, we find

$$V(s,\alpha) = -\frac{K a_0^2}{4 d_\perp} \sum_m (m d_\parallel + s) \frac{\sin \frac{2\pi}{d_\perp}\alpha}{\cosh \frac{2\pi}{d_\perp}(m d_\parallel + s) - \cos \frac{2\pi\alpha}{d_\perp}} \,. \tag{7.48}$$

The pinning potential has the same form as in Fig. 15 with, however, the energy barrier

$$\Delta E \sim K a_0^2 \frac{d_\parallel}{d_\perp} e^{-\pi d_\parallel / 2 d_\perp} \quad \text{for } \alpha = d_\perp/4 \,. \tag{7.49}$$

From Eqs. (7.47) and (7.49) we see that the energy barrier can vary from essentially zero to a value of the order of $k_B T$, depending on the ratio of $d_\parallel$ and $d_\perp$.

Let us now consider a situation where the vertical boundary is pinned symmetrically around the intersection with the horizontal grain boundary. We want to calculate the critical stress to depin the boundary at the intersection, assuming that it remains pinned at the two ends (see Fig. 16).

If no stress is applied, the grain boundary forms approximately two straight-line segments between the pinning centers. In general, these two segments will be tilted with respect to each other, if the intersection is a distance s away from the straight line joining the two pinned ends (see Fig. 16). The energy of this configuration in an applied stress field $\sigma_{ij} = \begin{pmatrix} 0 & \sigma \\ \sigma & 0 \end{pmatrix}$ can be found, using the methods of Sec. II:

$$\Delta E(s) = E(s) - E(0) = \frac{K a_0^2}{8\pi} \left[\frac{s}{d_\perp} \right]^2 - \tfrac{1}{2} \sigma a_0 s \frac{L}{d_\perp} + V_{\text{pin}}(s) \,. \tag{7.50}$$

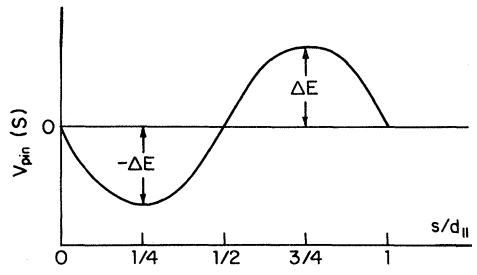

FIG. 15. Pinning potential of the vertical grain boundary of Fig. 14 as a function of s.

The first term gives the deformation energy if the shear stress is zero, and the second term is just the energy gain in a finite stress field σ,

$$\Delta E' = 2 a_0 \sum_{n=0}^{N_0/2} (b_i \epsilon_{jk} R_k^m \sigma_{ij}) \,, \tag{7.51}$$

where N_0 is the total number of dislocations in the grain boundary and $L = N_0 d_\perp$. Higher-order terms in σ have been neglected in (7.50). In the limit $d_\perp << d_\parallel$ the pinning potential $V_{\text{pin}}(s)$ is given by (7.48) and is approximately equal to

$$V_{\text{pin}}(s) = +\frac{K a_0^2}{4 d_\perp} \frac{s - s_0}{\cosh(2\pi/d_\perp)(s - s_0)} \,, \tag{7.52}$$

where α has been chosen as $\alpha = d_\perp/4$ and s_0 denotes the minimum of the potential well. Substituting (7.52) into (7.50) we find for the total energy

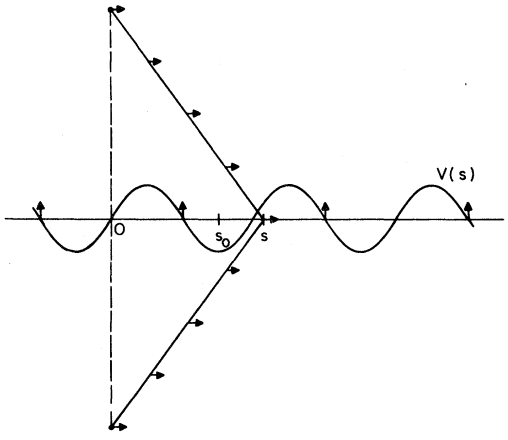

FIG. 16. Deformation of a pinned vertical grain boundary under an applied stress field and in the periodic potential $V(s)$ of an intersecting grain boundary.

$$\Delta E(s)=\frac{Ka_0^2}{8\pi}\left[\left[\frac{s}{d_\perp}\right]^2-\frac{4\pi\sigma L}{Ka_0}\frac{s}{d_\perp}+2\pi\frac{s-s_0}{d_\perp}\frac{1}{\cosh 2\pi(s-s_0)/d_\perp}\right]. \tag{7.53}$$

Clearly the determing parameter is

$$\Lambda=4\pi\sigma L/Ka_0\ . \tag{7.54}$$

$\Delta E(s)$ is plotted for various Λ in Fig. 17. Only for $\Lambda \gtrsim 1$ can thermal activation and nonlinear stress-strain relaxation occur. If we take the critical strain of the experiment of Ref. 6 we find that the grain size L must be roughly 10^5 Å.

There can be a distribution of values of $\alpha/d_\perp$ and $d_\perp/d_{||}$ so that nonlinear behavior can occur for any stress however small. Note that this critical stress ($\sigma_c \sim Ka_0/L$) is much smaller than the critical stress to remove dislocations from a grain boundary ($\sigma_c \sim Ka_0/d$). A widely separated dislocation pair ($d \sim L$) has a similar critical stress, and the barrier height is in both cases proportional to the sample thickness. Thus characteristic times will depend exponentially on the number of layers. But the widely separated dislocation pair just renormalizes the shear coefficient, while the gliding grain boundary will reduce the shear coefficient to zero.

VIII. APPLICATION TO MULTILAYER SMECTIC-B FILMS

In the previous sections we have examined the stability and time-dependent response of defect structures in a two-dimensional solid. We shall now discuss the application of these results to experiments in smectic films of two or more layers.

We shall be concerned here with dislocations and grain boundaries that penetrate all of the layers. If the coupling between layers is sufficiently weak, one should also consider the possibility of dislocations or grain boundaries restricted to a single molecular layer. The widespread occurrence of such single-layer defects would destroy interlayer correlations in the positions of the molecules, and would be contrary to the long-range order observed in x-ray experiments. The x-ray experiments do not rule out the existence of single-layer defects in some regions of the film, however, provided that large parts of the film are defect free.

From a theoretical point of view, a grain boun-

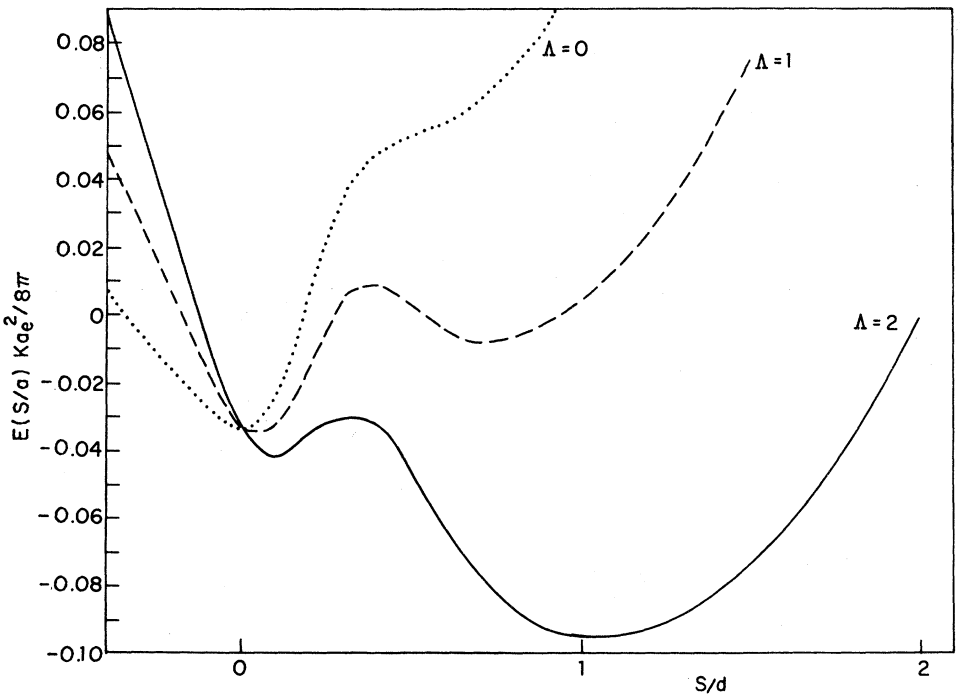

FIG. 17. Pinning potential of a vertical grain boundary *including* the elastic deformation energy for various values of $\Lambda=4\pi\sigma/Ka_0$. Depinning is possible for $\Lambda \gtrsim 1$.

dary or an array of dislocations confined to a *single* layer would appear to be less stable than a corresponding structure involving all the layers. For example, as a result of the coupling between layers, the attractive force between two dislocations of opposite sign in a single layer will not decrease to zero when the separation becomes large. Thus, if the climb diffusion constant is nonzero, the pair will tend to annihilate in a relatively short time.[32]

In order to apply the results of the previous sections to dislocations passing through all the layers in a multilayer film, we must first ask how the various parameters depend on n, the number of layers in the film. The force on a dislocation due to a strain of given magnitude, the energy of interaction between dislocations of fixed separation, and the elastic constants, measured in units of energy per unit area, should all be proportional to the thickness of the film. The mobilities $\gamma_{\perp}^{-1}$ and $\gamma_{||}^{-1}$, which relate the drift velocity of the dislocation to the total force on the dislocation, would be inversely proportional to the film thickness, for films of a few atomic layers. It follows that for processes in which the dislocation motion monotonically reduces the potential energy, the relaxation rate should be independent of n when the applied strain and the initial positions of the dislocations are specified. On the other hand, for processes requiring *thermal activation* over a barrier, such as the pair relaxation discussed in Sec. II D, there will be a marked decrease in relaxation rates for thicker films, as the energy barrier is proportional to n.

The relaxation of stress due to isolated pairs, where the separation of a pair is small compared to the distance between pairs, will only lead to a finite reduction of the shear modulus of the system. One can imagine, however, that a two-dimensional array of dislocations, composed of equal numbers of the different orientations of the elementary Burgers vectors, may have a series of configurations, each of which is locally stable with respect to glide, and such that one may pass from one configuration to another by gliding over a barrier, whose height is of the order of nk_BT_m. (We shall call this a *random neutral array* of dislocations.) There is likely to be a substantial distribution in these barrier heights, and we would expect to find a wide distribution in relaxation rates and nonexponential response to a change in stress.

In order for a "random" neutral array of dislocations to exist for times scales $\tau \gtrsim 10^3$ sec, the typical separation d between the dislocations must be $\gtrsim (a_0^2 \gamma_{\perp}^{-1} \mu \tau)^{1/2}$, where $\gamma_{\perp}^{-1}$ is the climb mobility and μ the shear modulus of the film. With our assumption that $D_{\perp} \approx 10^{-10}$ cm^2/sec for a single molecular layer and the shear modulus per layer approximately the Kosterlitz-Thouless value, we find $d \geq 10^5$ Å, independent of the thickness of the film. This would then imply a typical response time for nonactivated *glide* processes of order 10^{-1} sec. (This is slower than the experimental value, but not unreasonable in view of the crudeness of our estimates.) The rate for a "typical" thermally activated process would be reduced by a factor of order $e^{-0.6n}$, where n is the number of layers in the film. (The factor 0.6 in exponent is applicable to the example of the isolated pair studied in Sec. II D.)

The criterion for a factor-of-2 nonlinear enhancement of the stress relaxation rate in a thermally activated process is roughly

$$fd > k_BT \ , \tag{8.1}$$

where f is the force on the dislocation. For a film of n layers, close to the bulk $B \rightarrow A$ transition temperature, this becomes

$$U_{12} \gtrsim (4\pi)^{-1} a_0 / nd \ . \tag{8.2}$$

The experimental data cannot be explained by a simple array of small-angle grain boundaries of a unique length L and dislocation separation d. We have seen that such grain boundaries will relax exponentially in an applied stress at a rate $\sim D_{||}/dL$, independent of film thickness, to a new configuration which relieves a fraction, of order 50% of the stress. Interpenetrating arrays of such grain boundaries, with a variety of scales for L and d, can provide a mechanism for relaxation of a larger fraction of the stress, in a process that may be represented as a sum of exponentials with a variety of time scales. Stability against climb, for a time $\tau \approx 10^3$ sec, requires that the separations between the various grain boundaries satisfy

$$L \gtrsim (D_{\perp}\tau)^{1/2} \approx 3 \times 10^4 \text{ Å} \ ,$$

according to the analysis of Sec. II C. For $d/L = 0.1$, this gives glide relaxation times $\geq 10^{-2}$ sec.

Energy barriers to grain boundary gliding, and exponentially activated relaxation processes, may occur at the points where grain boundaries of different types cross each other. These effects might lead to a thickness dependence of the relaxation time, which would otherwise be absent in the grain-boundary model. It should be noted here

that a description in terms of small-angle grain boundaries is only sensible if $d << L$. In the case $d \approx L$, it is more appropriate to think in terms of a *random neutral array* of dislocations, discussed earlier.

Stress relaxation at large-angle grain boundaries, by a process of the Zener type, was considered in Sec. III using the results of Ghahremani. This does not seem to be a good candidate for the observed relaxation in smectic films because the overall relaxation obtained was fairly small and because the time scale for relaxation was rather fast. The relaxations times for this process should not have a marked dependence on film thickness.

The occurrence of slip at the sample boundary, considered in Sec. VI, could give arbitrarily large reductions of applied shear stress. We found, however, that except for the case of exceptionally smooth boundaries, which would have to be circular to a tolerance of $<< 1$ μm, the estimated relaxation times are found to be too long compared with the experiments. Furthermore, this effect would give a simple exponential relaxation, at a rate that is relatively insensitive to film thickness.

In Sec. V, we considered the motion of free dislocations, or of radial small-angle grain boundaries, that might be required to relieve stresses induced by a boundary condition which tended to bend the crystal as it is formed inside the annulus (see Sec. IV). The relaxation rates found in Sec. V for this process were too fast to explain the experiments, and once again, the rate would be insensitive to film thickness.

Of the various processes considered in this paper, the thermally activated glide diffusion of dislocations over interaction barriers in a dilute "random neutral array" seems the most consistent with the qualitative features of the relaxation observed by Sprenger *et al.*[6] in smectic-*B* films.

ACKNOWLEDGEMENTS

The authors are very grateful to R. Pindak and D. Osheroff for extensive discussions of their experimental data prior to publication. Discussions with W. F. Brinkman, J. Hutchinson, D. Moncton, D. R. Nelson, R. J. O'Connell, and P. Pershan are also gratefully acknowledged. Comments on the manuscript received from Dr. Pindak and Dr. Nelson were particularly helpful. This work was supported in part by the NSF through the Harvard Materials Research Laboratory and Grants Nos. DMR 77-10120 and DMR 77-18329. One of the authors (A.Z.) acknowledges the support of a fellowship from the Deutsche Forschungsgemeinschaft.

---

*Present address.

[1]C. C. Grimes and G. Adams, Phys. Rev. Lett. 42, 795 (1979); C. Rosenblatt, R. Pindak, N. A. Clark, and R. B. Meyer, *ibid.* 42, 1220 (1979); H. Birecki and N. M. Amer, J. Phys. (Paris) Colloq. 40, C3-433 (1979); P. Pieranski, Phys. Rev. Lett. 45, 569 (1980).

[2]R. Pindak, D. J. Bishop, and W. O. Sprenger, Phys. Rev. Lett. 44, 1461 (1980); J. C. Tarczon and K. Miyano, *ibid.* 46, 119 (1981).

[3]D. E. Moncton and R. Pindak, Phys. Rev. Lett. 43, 701 (1979).

[4]J. M. Kosterlitz and D. J. Thouless, J. Phys. C 6, 1181 (1973); J. M. Kosterlitz and D. J. Thouless, in *Progress in Low Temperature Physics,* edited by D. F. Brewer (North-Holland, Amsterdam, 1978), Vol. VII B, p. 373.

[5]B. I. Halperin and D. R. Nelson, Phys. Rev. Lett. 41, 121 (1978); 41, 519 (1978); D. R. Nelson and B. I. Halperin, Phys. Rev. B 19, 2457 (1979); A. P. Young, *ibid.* 19, 1855 (1979).

[6]W. O. Sprenger, R. Pindak, and D. D. Osheroff (unpublished).

[7]A. Zippelius, B. I. Halperin and D. R. Nelson, Phys. Rev. B 22, 2514 (1980).

[8]F. R. Nabarro, *Theory of Dislocations* (Clarendon, Oxford, 1967); J. Friedel, *Dislocations* (Pergamon, New York, 1964).

[9]For a review on grain boundaries see S. Amelinckx and W. Dekeyser, in *Solid State Physics,* edited by F. Seitz, D. Turnbull, and H. Ehrenreich (Academic, New York, 1959), Vol. 8, p. 327.

[10]J. Frenkel, *Kinetic Theory of Liquids* (Clarendon, Oxford, 1946).

[11]See S. Amelinckx and W. Dekeyser, in *Solid State Physics,* Ref. 9, p. 436.

[12]J. O. Hirschfelder, C. F. Curtis, and R. B. Bird, *Molecular Theory of Gases and Liquids* (Wiley, New York, 1954).

[13]D. Frenkel and J. P. McTague, Phys. Rev. Lett. 42, 1632 (1979); R. Morf, *ibid.* 43, 931 (1979); F. F. Abraham, *ibid.* 44, 463 (1980); S. Toxvaerd, *ibid.* 44, 1002 (1980); J. Tobochnik and G. V. Chester (unpublished); J. P. McTague, D. Frenkel, and M. P. Allen, in *Proceedings of the Conference on Ordering in Two Dimensions, Lake Geneva, Wisconsin, 1980,* edited by S. Sinha (North-Holland, Amsterdam, 1980).

[14]H. K. Hardy and T. J. Heal, Prog. Metal Phys. 5, 143 (1954); D. Turnbull, in *Solid State Physics,* edited by F. Seitz, D. Turnbull, and H. Ehrenreich (Academic, New York, 1956), Vol. 3, p. 266; R. W. Cahn, in *Impurities and Imperfections,* edited by D. Turnbull *et al.*, (American Society for Metals, Cleveland, 1955), p. 41. See also S. Amelinckx and W. Dekeyser, in *Solid State Physics,* Ref. 9, p. 435.

[15]A. H. Cottrell, Trans. AIME 212, 192 (1958); R. Armstrong, I. Codd, R. M. Douthwaite, and N. J. Petch, Philos. Mag. 7, 45 (1962).

[16]A. H. Cottrell, *Dislocations and Plastic Flow in Crystals* (Oxford University Press, London, 1953).

[17]N. F. Mott, Proc. Phys. Soc. London B 64, 729 (1951).

[18]A similar problem in three dimensions—the effect of a pinned dislocation line on the elastic constants—has been treated by J. S. Koehler, in *Imperfections in Nearly Perfect Crystals,* edited by W. Shockley *et al.* (Wiley, New York, 1952), p. 197.

[19]W. T. Read and W. Shockley, Phys. Rev. 78, 275 (1950).

[20]D. S. Fisher, B. I. Halperin, and R. Morf, Phys. Rev. B 20, 4692 (1979).

[21]The pinning of dislocation lines by defects in three dimensions is discussed by A. H. Cottrell, in *Plastic Deformation of Crystalline Solids* (Mellon Institute, Pittsburgh, 1950); P. Coulomb and J. Friedel, in *Dislocations and Mechanical Properties of Crystals,* edited by J. C. Fisher (Wiley, New York, 1957). 1957).

[22]A similar mechanism for dislocation lines in three dimensions is discussed in *Theory of Dislocations,* Ref. 8, p. 288.

[23]Motion of grain boundaries in three dimensions has been discussed by many authors, for example, R. Smoluchowski, in *Imperfections in Nearly Perfect Crystals,* edited by W. Shockley *et al.* (Wiley, New York, 1952), p. 451; J. E. Burke and D. Turnbull, Prog. Met. Phys. 3, 220 (1952).

[24]C. Zener, Phys. Rev. 60, 906 (1941).

[25]Ghahremani expresses his results in terms of the variable $r=r_2/(1+r_2)$. The quantity r is the three-dimensional Poisson ratio for these grains, which are constrained to have zero strain in the z direction.

[26]C. Zener, Phys. Rev. 60, 906 (1941). For a treatment of a random array of high-angle grain boundaries, see R. J. O'Connell and B. Budiansky, J. Geophys. Ref. 82, 5719 (1977).

[27]L. D. Landau and E. M. Lifshitz, *Theory of Elasticity* (Pergamon, New York, 1970).

[28]S. Amelinckx and W. Dekeyser, in *Solid State Physics,* Ref. 9, p. 442.

[29]The possibility that a fluid might exist at the boundary of a smectic-*B* film, and that the transport through such a fluid might be an important relaxation mechanism in a shear measurement, under some circumstances, was pointed out to us by D. Osheroff.

[30]Our discussion follows closely the work of Ambegaokar *et al.* on the nucleation of vortices in superfluid films [V. Ambegaokar, B. I. Halperin, D. R. Nelson, and E. D. Siggia, Phys. Rev. Lett. 40, 783 (1978); Phys. Rev. B 21, 1806 (1980)].

[31]S. Amelinckx and W. Dekeyser, in *Solid State Physics,* Ref. 9, p. 399.

[32]See, for instance, S. Hikami and T. Tsuneto, Progr. Theor. Phys. 63, 387 (1980).